SUB | NIEDERSÄCHSISCHE STAATS- UND UNIVERSITÄTSBIBLIOTHEK GÖTTINGEN

Werk

Jahr: 1985
Kollektion: fid.geo
Signatur: 8 Z NAT 2148:58
Digitalisiert: Niedersächsische Staats- und Universitätsbibliothek Göttingen
Werk Id: PPN1015067948_0058
PURL: http://resolver.sub.uni-goettingen.de/purl?PPN1015067948_0058

LOG Id: LOG_0012
LOG Titel: Ray synthetic seismograms for complex two-dimensional and three-dimensional structures
LOG Typ: article

Übergeordnetes Werk

Werk Id: PPN1015067948
PURL: http://resolver.sub.uni-goettingen.de/purl?PPN1015067948
OPAC: http://opac.sub.uni-goettingen.de/DB=1/PPN?PPN=1015067948

Terms and Conditions

The Goettingen State and University Library provides access to digitized documents strictly for noncommercial educational, research and private purposes and makes no warranty with regard to their use for other purposes. Some of our collections are protected by copyright. Publication and/or broadcast in any form (including electronic) requires prior written permission from the Goettingen State- and University Library.
Each copy of any part of this document must contain there Terms and Conditions. With the usage of the library's online system to access or download a digitized document you accept the Terms and Conditions.
Reproductions of material on the web site may not be made for or donated to other repositories, nor may be further reproduced without written permission from the Goettingen State- and University Library.

For reproduction requests and permissions, please contact us. If citing materials, please give proper attribution of the source.

Contact

Niedersächsische Staats- und Universitätsbibliothek Göttingen
Georg-August-Universität Göttingen
Platz der Göttinger Sieben 1
37073 Göttingen
Germany
Email: gdz@sub.uni-goettingen.de

J Geophys (1985) 58:2–26

Journal of Geophysics

Ray synthetic seismograms for complex two-dimensional and three-dimensional structures

V. Červený
Institute of Geophysics, Charles University, Ke Karlovu 3, 121 16 Praha 2, Czechoslovakia

Abstract. In recent years, considerable progress has been made in studies of the lateral heterogeneities in the Earth's interior and of seismic sources situated in realistic inhomogeneous media. In connection with these studies, the role of the ray method and of its various modifications is becoming increasingly important. In this paper, ways of applying the ray method to the evaluation of high-frequency body wave synthetic seismograms and synthetic time sections in complex two-dimensional and three-dimensional laterally varying layered structures are discussed. Certain new developments in the ray theory, mainly dynamic ray tracing and the paraxial ray approximation, make these computations fast and effective, even in 3-D structures. Although the computations are only approximate and the ray method may fail partially or completely in certain situations, the ray concepts have been found very useful in many practical applications of great seismological interest. The paper explains the physical principles and the most important algorithmic steps in the computation of ray synthetic seismograms. Numerical examples of ray synthetic seismograms and ray synthetic time sections are presented.

Key words: Seismic waves – Synthetic seismograms – Ray method– Dynamic ray tracing – Paraxial ray approximation

1. Introduction

Recently, considerable attention has been devoted to the numerical modelling of high-freqeuncy seismic wave fields in complex 2-D and 3-D layered structures. Several procedures of evaluating high-frequency body wave synthetic seismograms in laterally inhomogeneous media have been proposed. These procedures have immediately found important applications in various seismological investigations.

This paper is devoted to the computation of synthetic seismograms by the ray method. The *ray method*, also called the *ray series method*, or the *ART (asymptotic ray theory) method*, was first used to study the propagation of high-frequency elastic waves in inhomogeneous media by Babich (1956), see also Babich and Alekseyev (1958), and independently by Karal and Keller (1959). It is the simplest, but very powerful, representative of high-frequency asymptotic methods. One of its great advantages is its universality, effectivity and conceptual clarity.

The ray method, however, is only approximate and can be applied only to smooth media in which the characteristic dimensions of inhomogeneities are considerably larger than the prevailing wavelength of the propagating wave. Moreover, it has some other limitations, even in smoothly varying media. The main limitation consists in its lower accuracy or even invalidity in singular regions of the ray field, such as the caustic region, the critical region, the transition zone between the shadow and illuminated region, etc. In spite of these limitations, computer programs for the evaluation of ray synthetic seismograms in complex structures are very useful in the interpretation of seismic data.

In the ray method, as in other high-frequency methods, the complete wave field is composed of contributions – *elementary waves* – such as the refracted waves, waves reflected from individual interfaces, converted waves, multiply reflected waves, etc. These elementary waves can be simply evaluated along individual rays. Each elementary wave may be specified by some numerical (or alphanumerical) code which describes the history of its rays. The numerical codes may be introduced in various ways. They may be generated automatically, semi-automatically or manually. For complex 2-D and 3-D models, the semi-automatic generation of numerical codes often seems to be very convenient. It consists of automatic (optional) generation of the most important waves, e.g. of the primary P and S reflections from all interfaces, including refractions and converted reflections. Other desirable elementary waves, such as multiply reflected waves, may then be added by manual generation.

The ray method offers the possibility of investigating the individual elementary waves separately from others. This fact is very important in practical applications, e.g. in the interpretation of data obtained by deep seismic sounding of the Earth's crust or in seismic prospecting.

The basic step in the evaluation of the seismic wave field of individual elementary waves consists in ray tracing. Many ray tracing algorithms are now available. Some of them, based on some simple approximation of the model, are very fast, but are not quite suitable for the evaluation of ray amplitudes and ray synthetic seismograms as they may generate false anomalies in the amplitude-distance curves. The more sophisticated algorithms, based on the numerical integration of the ray tracing system, can be used more safely, but are more time consuming. Thus, the suitability of any ray tracing algorithm depends on the seismological problem we are treating.

In the evaluation of vectorial complex-valued amplitudes of elementary waves in 2-D and 3-D layered structures, the most important part is the evaluation of geometri-

cal spreading. The geometrical spreading can be evaluated in several ways. The simplest (but not very accurate) way is to measure numerically the cross-sectional area of the ray tube. In 3-D computations, it is necessary to compute at least three rays corresponding to close ray parameters to determine numerically the cross-sectional area of the ray tube. The second way is based on the so-called dynamic ray tracing. Dynamic ray tracing plays a fundamental role not only in the evaluation of geometrical spreading, but in many other applications. For example, dynamic ray tracing is a very important step in the paraxial ray approximation, which provides us with the possibility of evaluating the travel-time field and the displacement vector not only directly on the ray, but also in its vicinity. Finally, in some simple types of media, the geometrical spreading can be evaluated analytically.

There are two main approaches to the evaluation of ray synthetic seismograms in 2-D and 3-D laterally varying layered structures. The first is based on two-point ray tracing, the second on the paraxial ray approximation. Both these approaches are described in the following sections. Some examples of computations will also be presented.

This paper explains only the most important physical principles of the ray synthetic seismogram computation. Any attempt to present all the relevant mathematical equations would increase the length of the paper inadmissibly. Moreover, all necessary equations can be found in the extensive paper by Červený (1985b). Owing to the extensive use of various matrix notations and to the application of several coordinate systems and transformation matrices, the resulting equations in that paper are very concise and understandable from a physical point of view, even in the case of an arbitrary multiply reflected wave in a 3-D layered structure. All the equations are expressed algorithmically; the expressions are specified to the last detail. They can thus be used directly for programming.

The literature devoted to the ray method is very extensive. In this paper, we shall refer mainly to recent papers devoted, directly or indirectly, to the computation of ray synthetic seismograms in laterally varying layered structures. For a detailed treatment of many other aspects of the elastodynamic ray series method and of its applications in seismology, see the books by Červený and Ravindra (1971), Achenbach (1973), Červený et al. (1977), Goldin (1979), Aki and Richards (1980), Hubral and Krey (1980), Gerasimenko (1982). The ray series method has also been widely used in other branches of physics, mainly in electromagnetic theory. See, e.g. Kline and Kay (1965), Babich and Buldyrev (1972), Felsen and Marcuvitz (1973), Kravtsov and Orlov (1980).

Some attention in seismology has recently been devoted to the possibilities of the *space-time ray method.* In the space-time ray method, the wave field propagates along certains space-time, four-dimensional trajectories, called space-time rays. Their spatial projections are standard rays. The space-time rays may be easily computed, similarly to the space rays. The space-time ray-tracing systems and the space-time dynamic ray-tracing systems can be found e.g. in Kirpichnikova and Popov (1983). The space-time ray method may be applied to solve some elastodynamic problems in media with boundary conditions dependent on time (reflections from moving bodies), to study the propagation of high-frequency seismic waves in dispersive and slightly dissipative media, to study surface waves in laterally varying layered structures, to perform the downward and upward continuation of the seismic wave field, etc. In principle, the method could be easily applied even to the computation of synthetic seismograms. The author, however, is not aware of any attempt in this field. For this reason, we shall not discuss the space-time ray method in this paper. For more details and references, see Babich (1979), Kravtsov and Orlov (1980), Červený et al. (1982), Kirpichnikova and Popov (1983) and mainly the up-to-date monograph by Babich et al. (1985).

2. Ray tracing

Ray tracing has found broad applications in the solution of both direct and inverse seismological problems of laterally varying 2-D and 3-D layered media. In the numerical modelling of seismic wave fields, it plays an important role not only in the ray method itself, but also in many other more sophisticated high-frequency asymptotic methods. In these methods, the rays are used as a coordinate frame and the amplitudes are evaluated along rays in the new coordinate frame by more accurate methods than in the standard ray method. Examples are the extended WKBJ method, the Chapman-Maslov method, the Kirchhoff integral method, the method of Gaussian beams, etc. For more details and many references, see Červený (1985a) and Chapman (1985) in this volume. Ray tracing has found important applications even in surface wave studies. In the inverse methods, ray tracing is the basis of many recent inversion procedures (tomographic methods, various linearization approaches).

The ray tracing system in a 3-D smoothly varying medium consists of six ordinary differential equations of the first order. Three equations yield the ray trajectory (Cartesian coordinates of points along the ray) and the other three give the Cartesian components of the slowness vector at each point on the ray. Together with the computation of the ray trajectory, the travel time τ along the ray is also evaluated. The ray tracing system, with proper initial conditions, can be solved numerically by standard numerical techniques such as the Runge-Kutta method or by the predictor-corrector method. Some combinations of numerical and analytical methods may also be suitable for solving the ray tracing system; e.g. see Dobrovol'skiy and Fridman (1980) and Fridman (1983) for the method based on the Richardson extrapolation. *Initial-value ray tracing* is fast and stable and its accuracy can be easily controlled, even in the case of rays of multiply reflected, possibly converted waves. The new initial conditions for the ray tracing system at points of reflection/transmission at curved interfaces can be simply determined using Snell's law. Note that the initial-value ray tracing is also sometimes called Cauchy ray tracing.

The ray tracing systems can be written even for inhomogeneous *anisotropic* media. The initial-value ray tracing in an inhomogeneous anisotropic medium can be performed in the same way as in inhomogeneous isotropic medium, but it is more time consuming. For ray tracing systems in inhomogeneous anisotropic media, see Babich (1961), Vlaar (1968), Červený (1972), Červený et al. (1977), Petrashen and Kashtan (1984), Červený and Firbas (1984).

In seismological applications, however, we often need *boundary-value ray tracing.* The well-known example of boundary-value ray tracing is the so-called two-point ray

tracing, or source-to-receiver ray tracing. Assuming a point source, the rays are specified by the initial and endpoints of the ray (source and receiver). Instead of the initial point, some other boundary conditions may be important in certain applications. As an example, let us consider the computation of synthetic time sections in seismic exploration by the "normal ray" algorithm. In this case, the initial point of the ray is not specified. Instead, it is required that the initial direction of the ray be perpendicular to the reflector. Similar boundary conditions may be imposed if we start the computation from some initial surface. Boundary-value ray tracing is considerably more complicated than initial-value ray tracing, mainly in 3-D media. It can be performed in several ways. We shall briefly describe two such methods. The first method, called the *shooting method*, exploits Cauchy ray tracing. An iterative loop, in which the initial conditions for the ray tracing system are changed, is used to find the ray which passes through the receiver point. The initial conditions, which are changed in the shooting method, may have different physical meanings in various problems. In source-to-receiver ray tracing, they specify the initial direction of the ray at the source. In synthetic time-section computatons, they specify the position of the initial point on the reflector (the initial direction of the ray, perpendicular to the reflector, is then automatically determined). Various approaches can be used to change the initial conditions for a new iteration. Among others, it is possible to apply the recently proposed methods of the paraxial ray approximation, see Červený et al. (1984). Special care must be devoted to multiple arrivals of the wave under consideration (loops in the travel-time curves) and to the rays in certain singular regions of the ray field.

The second method, usually called the *bending method*, does not exploit standard ray tracing. In this method, an initial ray path is guessed and the perturbed iteratively to satisfy the appropriate differential equations.

For more details regarding boundary-value ray tracing, see Wesson (1971), Chander (1975), Julian and Gubbins (1977), Pereyra et al. (1980). A good review with many references can be found in Lee and Stewart (1981).

Both methods have their advantages and disadvantages. The shooting method is usually more cumbersome and time consuming than the bending method, especially in three-dimensional computations. If, however, the iterative loop is properly organized, it safely determines the rays of all required elementary waves arriving at the receiver position. If the elementary wave has several branches, e.g. in the case of loops in the travel-time curves, it determines all relevant multiple arrivals. Such rays may be easily lost in the bending method which has a tendency to determine only one of the multiple arrivals. For this reason, when computing synthetic seismograms or synthetic time sections for complex 2-D or 3-D layered structures, the shooting method or its various modifications have usually been used.

In most algorithms of high-frequency body wave synthetic seismogram computation, boundary-value ray tracing must be used. In some recent approaches, however, boundary-value ray tracing is not necessary. This applies, e.g. to the algorithms based on the paraxial ray approximation and on Gaussian beams. Both these algorithms only require initial-value ray tracing, which is fast, easy and simple. Even in these algorithms, however, it is useful to modify the initial-value ray tracing procedure. These algorithms require a system of rays with a sufficient density of endpoints in the vicinity of receivers. The density of endpoints must, of course, be higher for higher frequencies. A sufficient density of endpoints of rays is not always guaranteed by initial-value ray tracing in laterally varying complex structures. Some elementary waves may be overlooked, particularly if all the rays of these waves are within a very narrow pencil of rays from the source. This is the typical case of slightly refracted waves, similar to head waves. Often, the ray field of some elementary wave is very sparse in some region, although it is rather dense in another region. If the number of computed rays is increased considerably, the density of rays remains small in the former region and becomes unnecessarily high in the latter region.

A new method of ray tracing is proposed to deal with such situations. We call it *interval ray tracing*. Interval ray tracing is the ray tracing procedure in which it is required that at least the endpoint of one ray of the elementary wave under consideration is situated in any illuminated interval of specified length along the profile. If the elementary wave under consideration has several branches, the above requirement applies to any branch. In 3-D computations, instead of the length interval we use the surface element of a specified area.

The algorithm of 2-D interval ray tracing is as follows. The standard initial-value ray tracing is performed as long as the density of the endpoints is sufficient. If any given length interval is left out (i.e. no ray has its endpoint in that interval), an iterative loop is used to find at least one ray with the endpoint in that interval (if it exists). After this, the initial-value ray tracing continues with the original step.

A safe and general interval ray tracing routine for an arbitrary elementary wave in a 2-D laterally varying layered structure is now available. The algorithms for 3-D interval ray tracing are under investigation.

An example of the 2-D interval ray tracing is presented in Fig. 1. The model of the Earth's crust used in this example (model Zurich) will be described in more detail in Section 11, see Fig. 7. The shot point $x = 320$ km is considered, and three ray diagrams of the reflected PP wave from the intermediate crustal interface are shown. The first two ray diagrams are computed by standard initial-value ray tracing, and the third by interval ray tracing. In the first diagram, the step in the radiation angle is 1.8° (50 rays over the range from 0° to 90°). In the second diagram, the step is four times less, i.e. 0.45° (200 rays). As we can see in both these ray diagrams, the endpoints of the rays are distributed along the profile very irregularly. They are very dense close to the source and extremely sparse at larger distances from the source. At larger epicentral distances, there are practically no endpoints at all. The four-fold increase of the number of computed rays (from 50 to 200) added many superfluous rays at small epicentral distances, but only one ray with an endpoint beyond $x = 400$ km. The regular ray field, however, extends to a distance $x \sim 500$ km, see the last diagram computed by interval ray tracing. Interval ray tracing was performed with a basic step of 1.8° in the radiation angle, the same as in the first diagram. Nevertheless, the coverage of the profile by ray endpoints is considerably more regular than in the first and second diagrams. There are no "blind" regions along the profile. Note that interval ray tracing sometimes yields some rays situated very close to other rays. This case, however, can be easily treated in the synthetic seismogram algorithm.

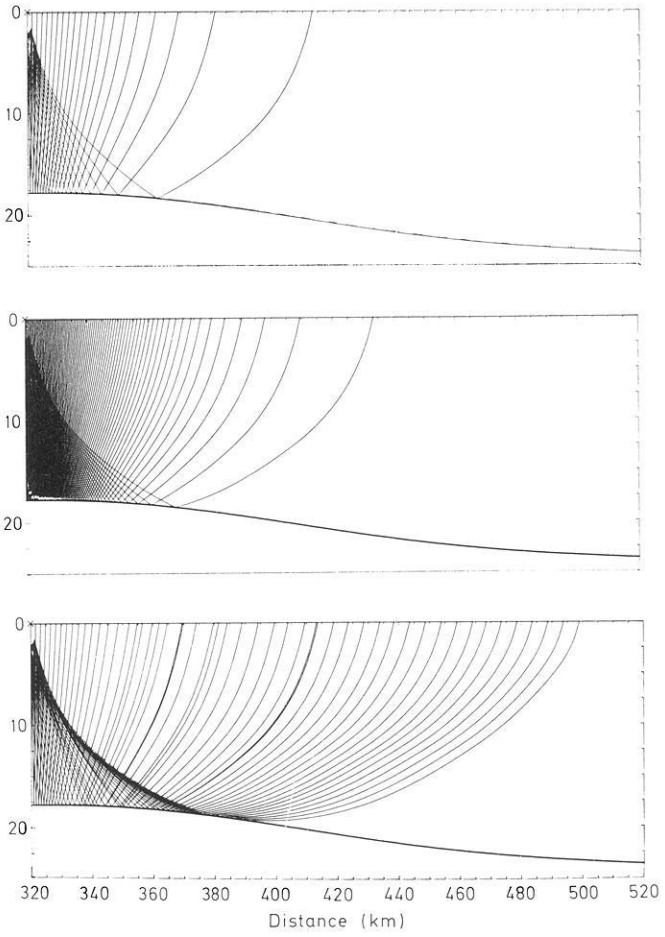

Fig. 1. Comparison of ray diagrams computed by initial-value ray tracing and by interval ray tracing. *Top diagram:* initial-value ray tracing, the basic step in the radiation angle is 1.8°. *Middle diagram:* initial-value ray tracing, the basic step in the radiation angle is four times less, i.e. 0.45°. *Bottom diagram:* interval ray tracing, the basic step in the radiation angle is again 1.8°. Interval ray tracing gives a more regular distribution of endpoints of rays along the profile

The interval ray tracing algorithm can be exploited to find even the rays of slightly refracted waves. It is often very difficult to catch these rays by initial-value ray tracing.

The algorithm of the interval ray tracing described above may be modified in several ways. For example, the initial conditions for the ray tracing system may be automatically varied in such a way as to obtain a required density of rays in the region of interest *using the results of the dynamic ray tracing*, see Section 5. In particular, the geometrical spreading matrix **Q**, defined in Section 4, plays a very important role in the algorithm. Such an algorithm of interval ray tracing may find applications mainly in 3-D computations, see Section 14 and also Červený (1985a).

The ray tracing system may be easily rewritten and solved numerically in any orthogonal coordinate system (spherical, cylindrical, etc.). For the very important case of a spherical coordinate system see, e.g., Jacob (1970), Julian and Gubbins (1977), Comer (1984).

In several simpler types of media, the ray tracing system can be solved analytically. This applies, e.g., to the case when the velocity V (or $1/V$ or $1/V^2$ or $\ln V$) is a linear function of Cartesian coordinates. The simplest analytical solution is obtained when the quantity $1/V^2$ (not V) changes linearly with the coordinates. The most popular analytical solution corresponds to the case when the velocity V changes linearly with coordinates. The ray trajectory is circular in such a medium and can be simply and efficiently calculated. For example, in the reflection methods of seismic prospecting, the commonly used model is composed of layers separated by curved interfaces, with a constant velocity or with a linear change of velocity within the individual layers. For more details and many references see Hubral and Krey (1980) and also Yacoub et al. (1970), Sorrels et al. (1971), Shah (1973a). This approximation has recently found applications even in seismology, see Lee and Langston (1983a, b), Langston and Lee (1983), Matveeva (1983).

In realistic models, it is sometimes complicated to describe the velocity distribution in the whole structure (or in the whole layer) by a simple analytical function. Often, however, the medium is divided into parts (blocks, tetrahedrons) with a simple analytical velocity distribution inside the individual parts. For example, let us assume that a smooth velocity distribution is specified in a regular or irregular network of points. It is then possible to divide the whole medium into tetrahedrons whose apexes are at the above points, and to use a linear approximation of V (or $1/V$ or $1/V^2$ or $\ln V$) in any of the tetrahedrons. The velocity then remains continuous across the boundaries of the individual tetrahedrons, but the gradient of the velocity changes discontinuously. In this way, second-order interfaces are generated. Unfortunately, these second-order interfaces produce some anomalies in the ray amplitude computations. For examples, see Červený (1985a). This approximation may thus be useful in travel-time computation, but it is not quite suitable for computing ray synthetic seismograms, unless some smoothing of amplitudes is used.

Most commonly, the linear approximation of V is used inside the tetrahedrons (or within triangles in 2-D computations). The segment of a ray inside any tetrahedron is again circular. Thus, the ray is evaluated as a succession of circular segments. The method has found important applications in seismology, mainly in seismic studies of crustal structure. See, e.g., Gebrande (1976), Will (1976), Whittall and Clowes (1979), Aric et al. (1980), Marks and Hron (1980), Cassell (1982), Müller (1984), Chapman (1985).

3. Polarization vectors

For any selected ray Ω, we can introduce the *ray-centred coordinate system* q_1, q_2, q_3 connected with Ω in the following way: One coordinate, say q_3, corresponds to the arc length s along the ray Ω, measured from an arbitrary reference point. The coordinates q_1, q_2 form a 2-D Cartesian coordinate system in the plane perpendicular to Ω at q_3, with its origin at Ω. This Cartesian coordinate system may be chosen in many ways. We shall choose it is such a way as to make the ray-centred coordinate system q_1, q_2, q_3 orthogonal. This condition determines the ray-centred coordinate system uniquely along the whole ray Ω, once the 2-D Cartesian system q_1, q_2 has been specified at any point on the ray. The ray-centred coordinate system was first introduced to seismology by Popov and Pšenčík (1978a, b).

The vector basis of the ray-centred coordinate system connected with Ω is formed at an arbitrary point O_s on

Ω by a right-handed triplet of unit vectors $\mathbf{e}_1(s)$, $\mathbf{e}_2(s)$, $\mathbf{t}(s)$, where $\mathbf{t}(s)$ is the unit tangent to the ray Ω at O_s and the vectors $\mathbf{e}_1(s)$, $\mathbf{e}_2(s)$ are perpendicular to Ω at O_s. For the orthogonal coordinate system connected with Ω, the unit vectors $\mathbf{e}_1(s)$, $\mathbf{e}_2(s)$ are strictly determined at any point on the ray Ω once they have been specified at some reference point of the ray.

It should be emphasized that the orthogonality of the ray-centred coordinate system means more than the mutual perpendicularity of $\mathbf{e}_1$, $\mathbf{e}_2$, $\mathbf{t}$ along the ray Ω. In any coordinate system ζ_i, $i=1, 2, 3$, we can express the square of the infinitesimal length element ds in the following way: $ds^2 = g_{ij} d\zeta_i d\zeta_j$, where g_{ij} are the components of the metric tensor corresponding to the coordinate system ζ_i. The coordinate system is called orthogonal if $g_{ij}=0$ for $i \neq j$ in the whole space. This is the case for the ray-centred coordinate system introduced here. The unit vectors $\mathbf{n}$, $\mathbf{b}$, $\mathbf{t}$, where $\mathbf{n}$ is the unit normal and $\mathbf{b}$ the unit binormal to the ray, are also mutually perpendicular at any point on the ray Ω. It can, however, be easily proved that the coordinate system q_n, q_b, $q_3 = s$, connected with the triplet $\mathbf{n}$, $\mathbf{b}$, $\mathbf{t}$, is not orthogonal for rays with a non-zero torsion.

The unit vectors $\mathbf{e}_1(s)$, $\mathbf{e}_2(s)$, $\mathbf{t}(s)$ play an important role in all high-frequency asymptotic methods of the investigation of seismic wave fields. Among others, they determine the direction of the displacement vector of high-frequency seismic body waves propagating in laterally varying layered structures. For this reason, these unit vectors are often called *polarization vectors*. More specifically, the unit vector $\mathbf{t}$ determines the direction of the displacement vector of P waves which is always linearly polarized. Especially important are the vectors $\mathbf{e}_1(s)$, $\mathbf{e}_2(s)$, as they determine the polarization of S waves. The S wave is generally elliptically polarized (although it may also be linearly polarized in some situations). The complex-valued displacement vector of S waves does not rotate with respect to $\mathbf{e}_1$, $\mathbf{e}_2$ as the wave progresses along Ω, although it rotates with respect to the unit normal $\mathbf{n}$ and unit binormal $\mathbf{b}$ to the ray. Thus, the polarization of S waves is determined by $\mathbf{e}_1$ and $\mathbf{e}_2$.

There are several ways of evaluating the unit vectors $\mathbf{e}_1$, $\mathbf{e}_2$ along the ray Ω in 3-D media. For example, they can be determined by just one simple auxiliary integration along the ray. For the relevant equations, see Popov and Pšenčík (1978a), Pšenčík (1979), Červený and Hron (1980), Červený (1985b). Cormier (1984) derived a relevant equation for rays expressed in spherical coordinates and used it to study the polarization of S waves propagating in laterally inhomogeneous models of the Earth's mantle (e.g. in lithosperic slabs).

In 2-D media, such computations are not necessary. One of the polarization vectors $\mathbf{e}_1$, $\mathbf{e}_2$ has a constant direction, and the other can be simply determined from the slowness vector. Similarly, the determination of polarization vectors $\mathbf{e}_1$ and $\mathbf{e}_2$ along the ray is straightforward in homogeneous media and in media in which V (or $1/V^2$) changes linearly with Cartesian coordinates. No integration along the ray is necessary to determine $\mathbf{e}_1$ and $\mathbf{e}_2$ in these cases.

4. Coordinate systems connected with rays. Transformation matrices

Besides the *general Cartesian coordinate system* x_1, x_2, x_3 and the *ray-centred coordinate system* q_1, q_2, q_3, it is convenient to introduce several other coordinate systems connected with rays and ray fields, mainly in 3-D computations. The application of various transformation matrices from one coordinate system to another simplifies the numerical modelling of high-frequency wave fields in complex structures considerably.

The ray coordinates γ_i ($i=1, 2, 3$) are not connected with one ray but with the whole ray field of the elementary wave under consideration. The quantities γ_1, γ_2 are parameters which specify individual rays and γ_3 is some parameter along the ray, e.g. the arc length s. The well-known examples of the ray parameters γ_1, γ_2 are the radiation angles in the case of a point source. In other situations, the ray parameters may have a different meaning, see e.g. Section 13.

Other useful coordinate systems are the *local Cartesian coordinate systems at points where the selected ray Ω impinges on interfaces*. They may be introduced to some extent arbitrarily. Generally, one coordinate axis coincides with the unit normal to the interface at the point of incidence, and one is perpendicular to the plane of incidence. A similar local Cartesian coordinate system may also be introduced at the endpoint of the ray.

All these coordinate systems can be specified by the transformation matrices from the system under consideration to the general Cartesian coordinate system x_i. These transformation matrices can be easily evaluated along Ω and play a basic role in the computation of the wave field, mainly in 3-D structures. For example, the transformation matrix from ray-centred to Cartesian coordinates along Ω is formed by Cartesian components of the polarization vectors $\mathbf{e}_1$, $\mathbf{e}_2$, $\mathbf{t}$. Thus, this transformation matrix is automatically obtained as a by-product of the computation of the polarization vectors.

The most important of these transformation matrices is the 2×2 transformation matrix $\mathbf{Q}$ from ray coordinates γ_1, γ_2 to ray-centred corodinates q_1, q_2; $Q_{IJ} = [\partial q_I / \partial \gamma_J]_{q_1 = q_2 = 0}$, $I, J = 1, 2$. The determinant of this transformation matrix can be used to evaluate the geometrical spreading. Therefore, this matrix can be called the *geometrical spreading matrix*. It can also be used to find the caustic points of the first and second order and to determine the index of the ray trajectory, also called the *KMAH index*. At caustic points of the first order, $\det\mathbf{Q} = 0$ and $\mathrm{tr}\mathbf{Q} \neq 0$. At caustic points of the second order, $\det\mathbf{Q} = \mathrm{tr}\mathbf{Q} = 0$. The geometrical spreading matrix can be evaluated by dynamic ray tracing, see that next section.

In certain applications, it may be convenient to introduce a special *phase space*, in which the coordinates correspond to the ray-centred components of the slowness vector, $p_I = \partial\tau / \partial q_I$. The 2×2 transformation matrix $\mathbf{P}$ from ray coordinates γ_1, γ_2 to the phase-space coordinates p_1, p_2; $P_{IJ} = [\partial p_I / \partial \gamma_J]_{q_1 = q_2 = 0} = [\partial^2 \tau / \partial q_I \partial \gamma_J]_{q_1 = q_2 = 0}$, has a deeper physical meaning and importance in certain high-frequency methods, e.g. in the Maslov method. It can be evaluated by dynamic ray tracing, together with the geometrical spreading matrix.

The application of the transformation matrices allows us to write the expressions for the displacement vector of arbitrary multiply reflected waves propagating in any 2-D or 3-D laterally varying layered structure in a very compact form. For a detailed treatment of the individual transformation matrices and for their applicatons, refer to Červený (1985b).

5. Dynamic ray tracing. Paraxial ray approximation

Dynamic ray tracing is a powerful procedure which has recently found many applications in the numerical modelling of high-frequency seismic wave fields in complex structures. In seismological terminology, the dynamic ray tracing system can be interpreted as the *approximate ray tracing system for paraxial rays* (rays situated close to the central ray Ω), expressed in the ray-centred coordinates connected with Ω. It consists in solving a system of ordinary differential equations along a known ray Ω. The dynamic ray tracing system can be expressed in different ways.The most suitable form of the dynamic ray tracing system seems to be a system of linear ordinary differential equations of the first order. In 2-D computations, the system consists of two scalar equations, in 3-D computations of two matrix equations (for 2×2 matrices **Q** and **P**).

There are many important applications of dynamic ray tracing. We shall list several of them here. Some other applications of dynamic ray tracing will surely be discovered in the future; they may be even more important than those listed here (applications in inverse problems, in the linearization procedures, in seismic source studies, etc.).

The most important quantities which may be determined by the dynamic ray tracing are as follows:
(a) Matrix **Q** of geometrical spreading and transformation matrix **P** from ray coordinates γ_1, γ_2 to phase-space coordinates p_1, p_2; $p_I=\partial\tau/\partial q_I$. (b) Geometrical spreading, proportional to $(\det\mathbf{Q})^{1/2}$. (c) 2×2 matrix **M** of second derivatives of the travel-time field with respect to ray-centred coordinates q_K, $M_{IJ}=[\partial^2\tau/\partial q_I\partial q_J]_{q_1=q_2=0}$ ($I, J=1, 2$). Matrix **M** can be determined from transformation matrices **Q** and **P** using the relation $\mathbf{M}=\mathbf{P}\mathbf{Q}^{-1}$. Matrix **M** itself satisfies a non-linear matrix Riccati equation. As soon as matrix **M**, the velocity of propagation and velocity gradients are known at some point on the ray, the 3×3 matrix of second derivatives of the travel-time field with respect to Cartesian coordinates x_1, x_2, x_3 can be easily determined. (d) 2×2 curvature matrix **K** of the wavefront, $\mathbf{K}=v\mathbf{M}=v\mathbf{P}\mathbf{Q}^{-1}$. Matrix **K** itself again satisfies a non-linear ordinary differential equation of the first order, which can be simply obtained from the Riccati equation for **M**. (e) Paraxial travel times. (f) Paraxial rays. (g) Fresnel volumes and/or Fresnel zones. (h) Paraxial components of the displacement vector. (i) Gaussian beams.

The dynamic ray tracing procedure may also be used to perform approximate boundary-value ray tracing or interval ray tracing in the vicinity of the central ray and to find the analytical continuation of the travel-time field into shadow zones.

When the ray is incident at an interface (surface of discontinuous velocity), the matrices **Q**, **P**, **M** and **K** change discontinuously across the interface along the ray. The transformation of **Q**, **P**, **M** and **K** across an interface has played an important role in various seismological applications, as it is directly connected with the problem of calculating the amplitudes of seismic body waves propagating in a layered medium. Traditionally, considerable attention has been devoted mainly to the behaviour of the curvature matrix. As the curvature matrix **K** can be easily continued along the ray in certain simple types of media (homogeneous, constant velocity gradient), the curvature matrix can be efficiently evaluated even along a multiply reflected ray in a layered medium and may be used to determine the geometrical spreading. This method is sometimes called the "wavefront curvature method", "principle curvature method" or similar. Such methods found wide applications mainly in seismic prospecting. See, e.g., Alekseyev and Gel'chinskiy (1959), Gel'chinskiy (1961), Červený and Ravindra (1971), Deschamps (1972), Shah (1973b), Hubral (1979, 1980), Hubral and Krey (1980), Červený and Hron (1980), Ursin (1982a, 1982b). Lee and Langston (1983a), Gjoystdal et al. (1984).

In models with a more complex velocity distribution within the individual layers, the curvature method would require the non-linear ordinary differential equation of first order for **K** to be solved along the ray. In this case, it is more useful and computationally more efficient to solve the linear dynamic ray tracing system for **Q** and **P**. The curvature matrix **K** may then be evaluated from **Q** and **P** at any point on the ray, but this is usually not necessary, matrices **Q**, **P** and **M** are sufficient to solve all problems of numerical modelling of high-frequency seismic body waves in complex structures.

Many papers have been devoted to various problems of dynamic ray tracing and/or to the evaluation of geometrical spreading. In addition to references given above, we mention several others: Belonosova et al. (1967), Červený et al. (1974), Green (1976), Červený (1976b). Popov (1977), Červený et al. (1977), Popov and Pšenčík (1978a, 1978b), Goldin (1979), Pšenčík (1979), Červený and Pšenčík (1979), Belonosova and Cecocho (1979), Azbel et al. (1980), Grinfeld (1980), Popov and Tyurikov (1981), Červený (1981a, b), Pšenčík (1983). The complete treatment of this problem for arbitrary multiply reflected waves in a 3-D laterally varying layered structure can be found in Červený (1985b).

The main importance of dynamic ray tracing consists in its applications in the so-called *paraxial ray approximation*, see items (e) and (h) above. In the standard ray method, the travel time and the displacement vector are evaluated only along rays. Thus, if we wish to evaluate the wave field at any point S by the standard ray method, we must find the ray which arrives at this point (boundary-value ray tracing). In the paraxial ray approximation, however, we need not evaluate the ray which arrives at S, but we can use any point O_s, situated on an arbitrary ray Ω passing *close* to S, to evaluate the wave field at S. In this case, however, the dynamic ray tracing must be performed along Ω. The position of both points O_s and S may be specified in general Cartesian coordinates, see Červený and Pšenčík (1983).

In many applications, it is suitable to use the fundamental matrix of linearly independent solutions of the dynamic ray tracing system. As soon as the fundamental matrix is known, many high-frequency asymptotic computations reduce to simple matrix algebra. In 3-D problems, the 4×4 fundamental matrix consists of two 2×2 matrix solutions, one of them is the "plane wave" solution, and the other the "point source" solution. Similarly, in 2-D problems, the 2×2 fundamental matrix consists of two solutions, one of them is again the "plane wave" solution and the other the "line source" solution.

Dynamic ray tracing takes only a small fraction of the computer time that ray tracing takes. Moreover, dynamic ray tracing has to be performed even in the standard ray method to evaluate the geometrical spreading. In this way, all the other possible applications are obtained practically without any increase in computer time.

Dynamic ray tracing can be performed even in *inhomogeneous anisotropic media*. For concrete forms of the dynamic ray tracing system in general anisotropic media, see Hanyga (1982).

Let us add one note to the derivation of the dynamic ray tracing system. The dynamic ray tracing system can be derived in a very simple and straightforward way from the eikonal equation rewritten in ray-centred coordinates, see Červený (1985b). A more general approach, based on the Riemannian geometry, is also available. Consider a three-dimensional Riemannian space with the metric tensor $g_{ij}=v^{-2}\delta_{ij}$, where v is the propagation velocity and δ_{ij} the Kronecker symbol. Then the rays correspond to *geodesics* in this space, and the system of differential equations for the geodesic corresponds to the ray tracing system. Similarly, equations for the so-called *geodesic deviation* correspond to the dynamic ray tracing system. The differential equations for the geodesics and for the geodesic deviations have been known for a long time and are applicable to any curved n-dimensional Riemannian space, with an arbitrary metric tensor g_{ij}, see e.g. Synge and Schild (1952). These equations have been widely used in mathematical physics, mainly in the general theory of relativity, see e.g. Synge (1960), Misner et al. (1973). The equations for geodesics and for geodesic deviations may be directly applied to ray tracing and dynamic ray tracing in "curved spaces" of seismological interest, for which the Riemann (curvature) tensor can be evaluated. As an example, let us mention here the ray tracing and dynamic ray tracing along an arbitrarily curved surface. This may be needed in surface wave studies, in finite-source studies (ray tracing along a generally curved fault surface), etc. The evaluation of the Riemann tensor, however, is not in general an easy procedure. For some related discussions and applications see Sharafutdinov (1979), Young (1985).

6. Computation of amplitudes

In this section, we shall discuss only the amplitudes of the zero-order term of the ray series solution. The higher-order terms of the ray series may be important in investigating the "higher-order" waves, such as pure head waves, and in investigating the accuracy of the zero-order term. The higher-order terms, however, have not yet found wider applications in seismology. For details regarding the evaluation of higher-order terms of the ray series and regarding head waves, see Červený and Ravindra (1971). Most of the important seismic body waves in seismology and seismic prospecting, such as waves reflected from first-order discontinuities, refracted waves, etc., are "zero-order" waves in the terminology of the ray series solution. In the following, we shall call the amplitudes of the zero-order term of the ray series the *ray amplitudes,* or simply amplitudes. The ray amplitudes are inversely proportional to the geometrical spreading.

As geometrical spreading can be evaluated by dynamic ray tracing, we shall first discuss the evaluation of the *"spreading-free" amplitudes*, i.e. the ray amplitudes without the geometrical spreading factor.

The procedures for computing complex-valued vectorial spreading-free amplitudes in 2-D media are well-known. The equations can be simply written in a compact form, even for an arbitrary multiply reflected, possibly converted, wave in a laterally varying layered structure. Such equations can be written even for 3-D media, but they are more complicated. The complications are caused mainly by the different orientation of the polarization vectors and the local Cartesian unit vectors at points of reflection/transmission. Both components of the S vector generally become coupled at any point of reflection/transmission. In 3-D computations, it is very convenient to use the matrix notation and various transformation matrices. The matrix notation and the use of transformation matrices again allow us to write the equations for the complex-valued displacement vector of an arbitrary multiply reflected/transmitted P, S or converted wave in any 3-D laterally varying layered structure in a compact analytical form, see Červený (1985b). Instead of reflection/transmission coefficients, however, 3×3 reflection/transmission matrices must be used, in which the elements are the standard reflection/transmission coefficients. The compact analytical equations for the displacement vector can be used in various applications. For example, they can be used to study and prove various reciprocity properties.

In numerical computation of the spreading-free amplitudes, the compact analytical expressions for the spreading-free amplitudes are not necessary. The computations may be performed by a straightforward step-by-step algorithm, following the ray from one interface to another, and applying relevant transformations at individual points of reflection/transmission. See Pšenčík (1979), Hubral and Krey (1980).

The spreading-free amplitudes can be used not only in ray applications, but also in some other more sophisticated computations, e.g. in the method of Gaussian beams. In the Gaussian beam approach, the standard geometrical spreading is replaced by another complex-valued function, the complex-valued spreading.

Generally speaking, the computation of the complex-valued vectorial spreading-free amplitudes is not a complicated problem. The procedures are fast and efficient if the relevant rays are known.

In the case of a point source, the expressions for the ray amplitudes also contain the radiation patterns of the source. It may sometimes be more suitable not to include the radiation pattern in the amplitudes, but to take it into account only in the synthetic seismogram computations. See the detailed discussion in the next section.

As mentioned in the introduction, the accuracy of ray amplitudes is limited in the singular regions of the ray field, such as the caustic region, the critical region, the transition zone between the shadow and illuminated regions, etc. In some situations, the ray expressions may even be fully invalid. For example, in shadow zones the ray method yields zero amplitudes and, directly at caustics, infinite amplitudes. It should be emphasized that certain singular regions (such as the caustic and critical regions) are of great importance in seismological applications, as the amplitudes may be considerably large there. To evaluate the amplitudes in singular regions, various modifications of the ray method have been proposed. Well-known examples are the Airy modification in the caustic region, the Weber-Hermite modification in the critical region, etc. The references to the evaluation of the wave field in singular regions are too numerous to be given here. For a more detailed explanation and many references, see Babich and Buldyrev (1972), Fel-

sen and Marcuvitz (1973), Červený et al. (1977), Kravtsov and Orlov (1980), Červený (1981a), Klem-Musatov and Aizenberg (1984), Chapman (1985). Let us only note that the amplitudes of seismic body waves in singular regions are frequency dependent.

Another limitation of the ray method is as follows. Certain seismic waves cannot be described by the ray series method. Let us mention here various diffracted waves connected with corners and edges in interfaces, the grazing diffractions, waves which propagate at least partly along non-ray paths, such as screened waves, evanescent waves, tunnel waves, pseudospherical waves like S^*, etc. Some of these waves may be of importance in seismology and seismic prospecting. Similarly as in the preceding case, various modifications of the ray method have been proposed which can be used to find asymptotic high-frequency expressions for these waves. They again yield frequency-dependent amplitudes. These modifications can be simply included in the ray computations. A good example are the Klem-Musatov expressions for the edge waves (see Klem-Musatov and Aizenberg 1984), the asymptotic expressions for pseudospherical waves, etc. See again the references given above.

Moreover, the standard ray series method is not able to describe waves of an interference character, connected with very thin layers, whispering gallery waves, etc. For certain of these waves, some modifications of the ray method have again been proposed (e.g. for whispering gallery waves). Some other waves of the interference type may be evaluated by hybrid methods, which will be described in the next section.

As mentioned in Section 2, there is still one additional problem in the evaluation of ray amplitudes. The ray amplitudes of some body waves are very sensitive to minor details in the approximation of the medium, e.g. to artificial interfaces of second order, fictitious small oscillations of the velocity distribution, etc. There are two possibilities of avoiding this problem. First: it is possible to use an approximation of the medium which is smooth enough to suppress the artificial effects. Unfortunately, this is a very complicated problem, see Section 9. Another possibility is to smooth the computed ray amplitudes. One such possibility will be described briefly in Section 8. It would, of course, also be possible to use other methods of numerical modelling, which automatically include some smoothing, such as the Chapman-Maslov method (see Chapman 1985) or the method of Gaussian beams (see Červený 1985a, Section 12).

As the ray method is only approximate, it would be useful to have some possibility of estimating the error in the computation of amplitudes. Unfortunately, the *validity conditions* have usually only a qualitative, not quantitative, character. Therefore, it is not simple to give quantitative estimates of the error in ray amplitudes. The validity conditions, however, tell us when and where the error is larger (smaller). Usually, the accuracy of the ray method is studied quantitatively by the comparison of ray results with more exact computations for some canonical problems. For more details on the validity conditions, see Červený et al. (1977, Chapter 8), Ben-Menahem and Beydoun (1985a, b).

The ray method can be used to determine ray amplitudes of high-frequency seismic body waves even in more complicated types of media, such as anisotropic, prestressed, slightly dissipative, porous and random media.

7. Elementary wave quantities. Elementary seismograms

As soon as the travel times and vectorial complex-valued amplitudes of individual elementary waves are available, it is possible to evaluate elementary seismograms, i.e. the contributions of the individual elementary waves to the whole wave field in the time domain.

To determine the elementary synthetic seismograms, we must know the source-time function and its Hilbert transform. Various source-time functions have been used in synthetic seismology. Let us mention, e.g., the Berlage signal, the Ricker signal, Küpper's signal, etc. We prefer to use the Gaussian envelope signal (also called the Gabor signal)

$$F(t)=\exp[-(2\pi f_M(t-t_0)/\gamma)^2]\cos[2\pi f_M(t-t_0)+\nu],$$

where f_M, γ, t_0 and ν are real-valued free parameters. The signal corresponds to a harmonic carrier (frequency f_M) with a Gaussian (bell-shaped) envelope. For larger γ (say, $\gamma \gtrsim 2.5$), the signal has a very narrow amplitude spectrum, highly concentrated at frequency f_M. The Hilbert transform of $F(t)$ can then also be expressed analytically by means of an approximate equation, see Červený (1976a),

$$H(t)=-\exp[-(2\pi f_M(t-t_0)/\gamma)^2]\sin[2\pi f_M(t-t_0)+\nu].$$

This makes the evaluation of elementary seismograms very easy. Moreover, by a proper choice of the parameters f_M, γ, ν, t_0 we can simulate a large variety of seismic signals observed in seismology and in seismic prospecting.

The analytic expressions for the Hilbert transform are known for several other useful source-time functions; the most important of them is the delta function. In this way, we can easily construct the elementary seismograms for the delta source-time function. This source-time function, however, contains very low frequencies (including the D.C. component) which are not allowed in the high-frequency calculations. Nevertheless, the delta function computations may be performed, but the results must later be convolved with some high-frequency source-time function. For other details, we refer the reader to Červený (1985b).

If the source-time function is known, the elementary seismogram of any multiply reflected wave propagating in an arbitrary structure is fully specified at a receiver point by the following quantities: the travel time and the vectorial complex-valued amplitudes. We call these quantities the *elementary wave quantities*.

In a general 3-D medium if we are interested in all the three Cartesian components of the displacement vector, there are seven real-valued elementary wave quantities: the real-valued travel time and two real-valued numbers for each component of the displacement vector.

The number of elementary wave quantities may be decreased in some special situations. For example, in 2-D *P-SV* computations there are five elementary quantities, in 2-D *SH* computations there are three.

We have considered real-valued travel times. In some cases, it is suitable to consider complex-valued travel times. This applies, e.g., to slightly dissipative media. One additional elementary wave quantity, which corresponds to the imaginary part of the travel time, must then be considered.

In slightly dissipative media, it is convenient to include among the elementary wave quantities the so-called global absorption parameter

$$t^*=\int_{O_0}^{O_s}(VQ)^{-1}\,ds,$$

where Q is the quality factor and V is the velocity; the integration is taken along the ray from the source to the receiver. In addition to standard synthetic seismograms for a non-absorbing medium, elementary synthetic seismograms for various absorption models (including models of causal absorption) may then be constructed.

If the elementary wave quantities are known, the elementary synthetic seismogram can be computed for any high-frequency source-time function. The possibilities of elementary synthetic seismograms may be considerably generalized if some other additional quantities are available, together with the elementary wave quantities listed above. For example, in the case of a point source, it is useful also to store the two radiation (take-off) angles. The radiation patterns of the source need then be taken into account only in the elementary synthetic seismogram computations, not in the amplitude evaluation. The procudure is as follows: the amplitudes are evaluated for an isotropic radiation pattern of the source, and only the elementary synthetic seismograms are multiplied by the radiation pattern under consideration. In this way, the elementary synthetic seismograms may be calculated for various radiation patterns practically without any additional numerical effort.

The approach described may, however, be slightly more complicated in 3-D computations as the radiation patterns for the two components of S waves (e.g. SH and SV) are generally different. In this case, three other complex-valued Cartesian components of the displacement vector must be stored if the source generates an S wave. In 2-D computations, this increase of elementary wave quantities is not necessary as the two components of S waves are not coupled together.

8. Ray synthetic seismograms

By ray synthetic seismograms, we understand a superposition of the elementary seismograms of all elementary waves (or some selected elementary waves) arriving along various ray trajectories from the source to the receiver within a specified time window.

Much attention in the seismological literature has been devoted to the automatic generation of numerical codes of multiply reflected waves in horizontally layered media with homogeneous layers, see e.g. Hron (1972). In such media, the elementary waves may be effectively grouped into families of kinematic and dynamic analogs. Only a finite number of elementary waves arrives at the receiver within a specified time window in this case. In inhomogeneous layered structures, an infinite number of elementary waves may arrive at the receiver, even if a time window of finite length is considered. Thus, the ray synthetic seismogram cannot be generally complete, only partial ray expansion is possible. Moreover, in laterally varying layered structures, the elementary waves must be treated individually; they cannot be grouped into families of kinematic and dynamic analogs. The automatic generation of numerical codes would be more complicated in this case. The ray method is most effective in situations in which only a small number of elementary waves needs to be computed. A medium composed of thick layers separated by smooth interfaces, with a smooth velocity distribution inside individual layers, may serve as a good example; particularly if the epicentral distances of receivers are not too large. The problem of automatic, semi-automatic and manual generation of numerical codes of elementary waves was briefly discussed in Section 1.

The basic data file for the evaluation of ray synthetic seismograms is the file containing the set of elementary wave quantities, for all receivers and all elementary waves under consideration. As soon as this file is available, the evaluation of ray synthetic seismograms is easy and fast. In principle, three approaches can then be used to evaluate the ray synthetic seismograms:

a) Direct summation of elementary seismograms.

b) Frequency domain approach. In the frequency domain approach, the frequency response is evaluated first, using the elementary wave quantities of all elementary waves under consideration. Multiplying it by the spectrum of the source-time function yields the spectrum of the synthetic seismogram. Finally, the ray synthetic seismogram is evaluated by inverse Fourier transform.

c) Convolutory approach. First, the complex-valued impulse response is calculated. The source-time function corresponds to the delta function in this case. The ray synthetic seismogram is then obtained as the real part of the convolution of the complex-valued impulse response with the analytical signal corresponding to the source-time function. Several alternative approaches can be used. In some of them, it is not necessary to work with the analytical signal of the source-time function, but only with the real-valued source-time function. See Chapman (1985) for details.

All the above three approaches have certain advantages and disadvantages. If the number of elementary waves is small and the Gaussian envelope signal is considered as a source-time function, the approach based on the summation of elementary seismograms is the simplest and most straightforward. On the other hand, the frequency-domain approach is more general. If the number of elementary waves is large, it may even be faster. As the vectorial complex-valued amplitudes of elementary waves are independent of frequency in the ray method, a fast method can be used to evaluate the frequency response. The frequency response at any specified receiver has the following form:

$$X(f) \sum_{n=1}^{N} U^n \exp(i2\pi f \tau_n),$$

where f is the frequency, N is the number of elementary waves under consideration, τ_n is the travel time and U^n the relevant component of the vectorial complex-valued amplitude of the n-th elementary wave, and $X(f)$ is the spectrum of the source-time function. Both U^n and τ_n are independent of frequency. Assume that we evaluate the frequency response for frequencies f_k, $k=1, 2, \ldots, K$, with $f_{i+1}-f_i=\Delta f=\text{const}$. Then, for each elementary wave ($n=1, 2, \ldots, N$), the contribution $U^n \exp(i2\pi f \tau_n)$ must be evaluated for frequencies f_k, $k=1, 2, \ldots, K$. The most time-consuming step is the evaluation of trigonometric functions $\cos(2\pi f_k \tau_n)$ and $\sin(2\pi f_k \tau_n)$. The *fast frequency response (FFR) algorithm*, which removes the calculation of trigonometric functions, is as follows. For a given n, the contribution $U^n \exp(i2\pi f \tau_n)$ is directly evaluated only for the first frequency f_1. Then the quantity $A=\exp(i2\pi \Delta f \tau_n)$ is computed. For all other frequencies $f_k > f_1$, *only one complex-valued multiplication* is needed to evaluate $U^n \exp(i2\pi f_k \tau_n)$, as $U^n \exp(i2\pi f_k \tau_n) = U^n \exp(i2\pi f_1 \tau_n) A^{k-1}$. Thus, no trigonometric functions need be computed. The FFR algorithm can be used even for complex-valued τ_n (slightly dissipative media, Gaussian beams) and for certain cases of frequency-

dependent U^n [if $U^n = G(f)\,\tilde{U}^n$, where $\tilde{U}^n$ is frequency independent and $G(f)$ is the same for all n].

The frequency-domain approach also allows some frequency-dependent effects (dissipation, frequency characteristics of recording equipment, subsurface thin layering, thin transition layers, etc.) to be included simply in the computations. It also allows various modifications of the ray method to be considered in singular regions, and the non-ray waves, such as the diffracted, evanescent, pseudospherical, and higher-order waves, to be included. In most of these frequency-dependent effects, however, the fast frequency response (FFR) algorithm cannot be used. It can still be used in the case of non-causal absorption and even for certain causal absorption models, if the model is considered in linearized form, see Červený (1985a, b). Certain problems in the frequency-domain approach may be caused by the aliasing effect.

As mentioned in Section 1, ray synthetic seismograms may be evaluated by *two methods*. The first method is based on *boundary-value ray tracing* and was explained above. The second method is based on the *paraxial ray approximation*. In the second method, boundary-value ray tracing is not necessary, only initial-value or interval ray tracing is required. The initial-value or interval ray tracing does not yield the elementary wave quantities directly at the receivers, but in some irregular system of endpoints of rays along the Earth's surface. The system of endpoints must cover the region of interest D_0 with sufficient density. The receiver coordinates need not be specified at this stage, only the region of interest D_0 must be known.

The elementary synthetic seismogram can then be evaluated at any point S of region D_0 by the method of paraxial ray approximation. The knowledge of the elementary wave quantities at the endpoints of rays, however, it not sufficient to evaluate elementary synthetic seismograms at S, we must know some additional quantities. To compute elementary synthetic seismograms by the paraxial ray approximation at S, the following quantities must be stored at the endpoints of rays: the Cartesian coordinates of the endpoint, the Cartesian components of the slowness vector at the endpoint, the travel time, the spreading-free vectorial complex-valued amplitudes, the Cartesian components of the velocity gradient at the endpoint, the index of the ray trajectory (KMAH index) and the results of dynamic ray tracing. Optionally, we can again store the quantity t^* and the radiation angles.

If such a file is available, ray synthetic seismograms can be evaluated at any point of the region D_0. Only now need the coordinates of the receiver points be specified. In 3-D calculations, the receiver points may be distributed regularly or irregularly along various profiles.

Two algorithms based on the paraxial ray approximation may be used to evaluate the travel time and the complex-valued vectorial amplitude at a specified receiver point from the quantities stored at the endpoints of rays. In the first algorithm, the travel time and complex amplitude are determined at the receiver from the *nearest endpoint* of the ray. In the second algorithm, the travel time and complex amplitude at the receiver are obtained as a *weighted superposition* corresponding to several of the closest endpoints. The second algorithm automatically includes some smoothing which may be very useful in the ray amplitude computations. If Gaussian weighting is used to evaluate the ray amplitude at the receiver, the approach is in fact very close to a special case of the Gaussian beam summation method, see Červený [1985a, Eq. (18)].

The computation of synthetic seismograms by the ray method is most effective if we deal with a small number of rays only. As soon as the number of rays becomes very large, difficulties may appear. Firstly, the procedures become cumbersome if a large number of elementary waves must be evaluated. Secondly, certain principal difficulties can also be encountered in the case of destructive interference of waves. The leading terms of the individual waves may cancel each other. Various modifications were suggested to overcome these difficulties, e.g. hybrid ray-mode methods or hybrid ray-reflectivity methods. The latter modification is very convenient if the model is composed of thick smoothly inhomogeneous layers separated by thin transition layers with abrupt changes of velocity. The ray method can then be applied to the thick layers and the reflection/transmission coefficients at the individual interfaces are replaced by frequency-dependent reflection/transmission coefficients for the transition layers, evaluated by matrix methods. See Ratnikova (1973), Daley and Hron (1982).

The concrete algorithms for the computation of ray synthetic seismograms depend considerably on the purpose, required accuracy and completeness of computations, and are described in many papers publishing during the last few years. Several references will be given here for the reader's convenience.

Ray synthetic seismograms have found applications mainly in *seismic investigations of the Earth's crust*. In the 1960s the ray synthetic seismograms were evaluated for crustal models composed of parallel thick homogeneous layers (e.g., see Červený and Novák 1968). Several modifications of the ray method, such as the Weber-Hermite modifications in the critical region, were applied to increase the accuracy of ray computations. The programs were also modified for vertically inhomogeneous layered structures, simulating them by thin homogeneous layers (similar to the reflectivity method). Certain algorithms and programs, written at that time, such as program SEIS4, found broader applications in the interpretation of seismic crustal data. See the detailed expositions of these methods with many examples in the book by Červený et al. (1977). The evaluation of ray synthetic seismograms for general vertically inhomogeneous layered structures may be useful even at present. A new, very fast and efficient algorithm and program for such computation is described in Červený and Janský (1985). The ray method, of course, cannot compete in the accuracy of computations with the reflectivity method, but it is considerably faster and more efficient, at least for such structures in which the higher multiple reflections do not play a considerable role.

Ray synthetic seismograms, however, have found most natural applications in laterally varying layered crustal models (where the reflectivity method cannot be used). The first ray synthetic seismograms for 2-D crustal structures, mostly composed of homogeneous layers separated by curved interfaces, were computed at the beginning of the 1980, e.g. see Hron and Kanasewich (1971). The algorithms, details of computations and numerical examples can be found in Červený and Pšenčík (1977), Hron et al. (1977), Červený et al. (1977), Červený (1979), Marks and Hron (1980), McMechan and Mooney (1980), Cassel (1982), Spence et al. (1984). The accuracy and computer efficiency

of the ray synthetic seismogram was investigated in great detail by DeSisto and Smith (1983). See also Examples 2 and 3 in Sections 11 and 12 and other references therein. The comparison of computations by different algorithms for a 2-D laterally varying model of the Earth's crust, proposed by W.D. Mooney, was performed in the Workshop of the Commission on Controlled Source Seismology at Einsiedeln, 1983; for results, see Mooney (1985). The model, however, is not quite suitable for ray computations as it contains very thin layers and corner points in interfaces. Various modifications of the ray method may also be used to compute synthetic seismograms for 2-D layered structures. For example, the synthetic seismograms evaluated by the Wiggins disc theory are reported by Chiang and Braile (1984). Note that 2-D ray synthetic seismograms have even been computed for slightly dissipative media, see Krebes and Hron (1980, 1981), Červený and Pšenčík (1984), and for certain simpler types of anisotropic inhomogeneous media. For a review with many references, see Červený et al. (1980), Červený (1983), Fertig and Pšenčík (1985).

In interpreting seismic crustal measurements, 3-D laterally inhomogeneous layered structures have not yet been widely considered. At present, however, effective algorithms and program packages are available, which allow numerical modelling even in the case of 3-D crustal models. For details, see Červený et al. (1984), where also some numerical examples of ray synthetic seismograms for a 3-D crustal structure are presented. Generally speaking, the 3-D synthetic seismogram computations are not complicated, especially if the paraxial ray approximation is used. The 3-D computations are, of course, more time consuming than 2-D computations. There are some exceptions. If the receivers are not distributed over a 2-D region on the Earth's surface, but only along one roughly straight-line profile, and if the epicentre is situated close to that profile, the computation of the synthetic seismograms is very fast, even for 3-D models. The synthetic seismogram computations then do not require considerably more computer time than the computations for 2-D models. The distribution of receivers and sources described is typical for deep seismic sounding studies of the Earth's crust, so that 3-D synthetic seismogram computations can be performed in this case even on 200-K-size computers and require only a reasonable amount of computer time. See Example 5 in Section 14.

Recently, ray synthetic seismograms and synthetic time sections have found broader applications even in 2-D and 3-D numerical modelling of seismic wave fields in *seismic prospecting*. See, e.g., Hron et al. (1977), May and Hron (1978), Zilkha et al. (1983), Sierra Geophysics (n.d.), etc. For simple 2-D examples of synthetic seismogram and synthetic time-section computations for models of some interest in seismic prospecting refer to Sections 10 and 13. The author expects the importance of ray concepts and particularly of the ray synthetic seismograms in seismic prospecting, mainly in 3-D seismics, to increase considerably in the near future.

9. Approximation of the velocity distribution in the model

The approximation of the velocity distribution in 2-D and 3-D layered structures is not a simple problem. The amplitudes evaluated by the ray method are sensitive to some pecularities of the approximation, e.g. to artificial second-order interfaces, to small oscillations of the velocity distribution and to corners in interfaces, introduced by approximation methods. These small details in the approximation are often responsible for the anomalous behaviour of ray amplitudes in certain ranges of epicentral distances. For example, the bilinear approximation, or a piecewise linear triangular approximation generates such second-order interfaces. They are, therefore, not quite suitable for computing ray amplitudes and ray synthetic seismograms (although they may be useful in the evaluation of travel-time curves). The spline approximation does not generate such interfaces and is usually more useful. Unfortunately, the spline approximation may generate some small oscillations, which again cause anomalies in the ray field and in amplitude computations, mainly in regions of stronger changes of velocity. In deep seismic studies of the Earth's crust, this applies particularly to the uppermost part of the crust. It is more convenient to use smoothed splines or splines with tension.

Generally, the smooth approximation of the velocity distribution in 2-D and 3-D models is the most complicated part in the evaluation of ray amplitudes and ray synthetic seismograms. This is one of the reasons why such a large effort has been devoted recently to the investigation of more sophisticated high-frequency methods which would not be so sensitive to the minor peculiarities in the approximation of the velocity distribution.

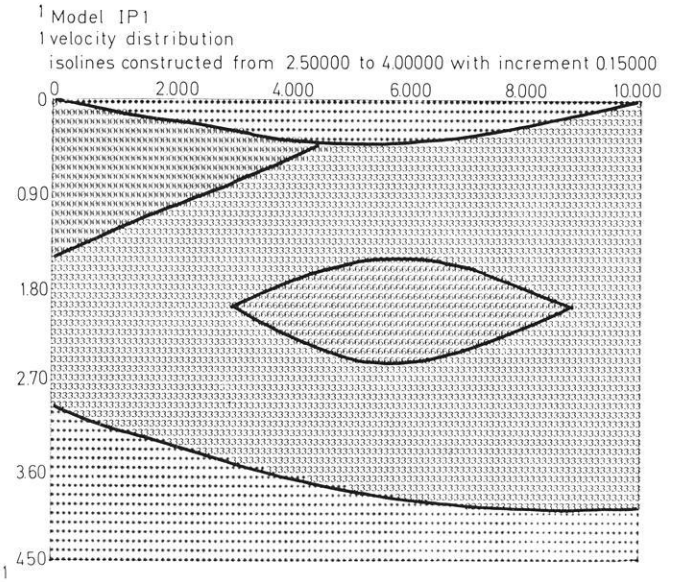

Fig. 2. The 2-D laterally varying model IP1, with a lens-like high-velocity body, used for the computation of the numerical example 1. The *P*-wave velocities in individual layers are constant

Fig. 3. Model IP1, shot point at $x = 5$ km. Examples of source-to-receiver ray diagrams, travel-time and ray amplitude-distance plots for two elementary primary reflected waves. *Bottom part:* ray synthetic seismograms of the vertical component (*left*) and horizontal component (*right*) of the displacement vector. No amplitude normalization is used; travel times are not reduced. All primary reflected waves, including converted waves, are considered

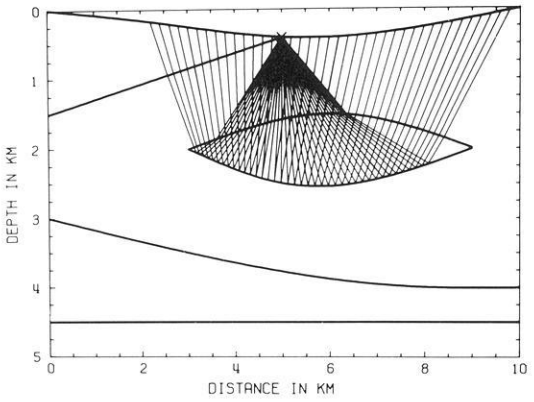

PP REFLECTED WAVE - 4TH INTERFACE

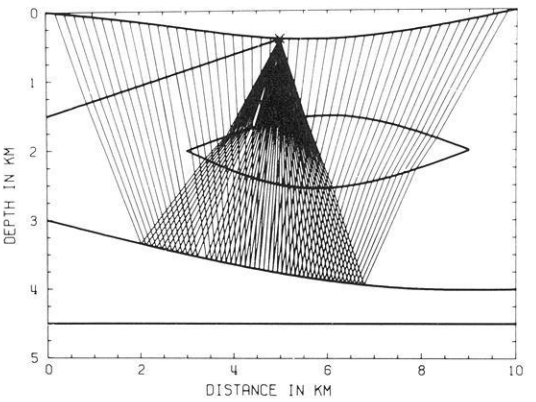

SS REFLECTED WAVE - 5TH INTERFACE

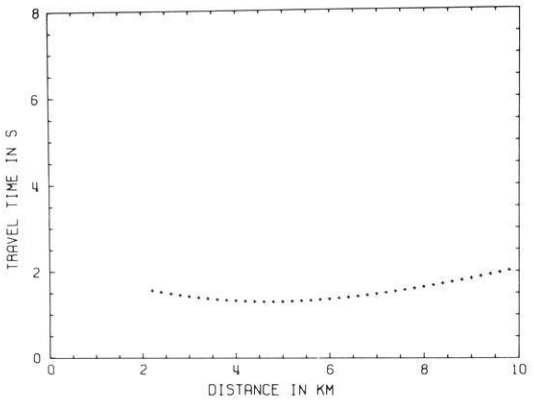

PP REFLECTED WAVE - 4TH INTERFACE

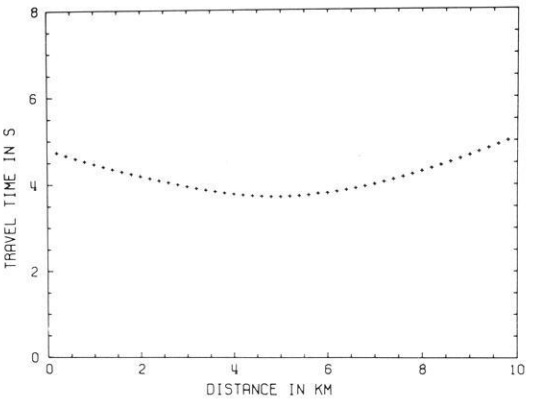

SS REFLECTED WAVE - 5TH INTERFACE

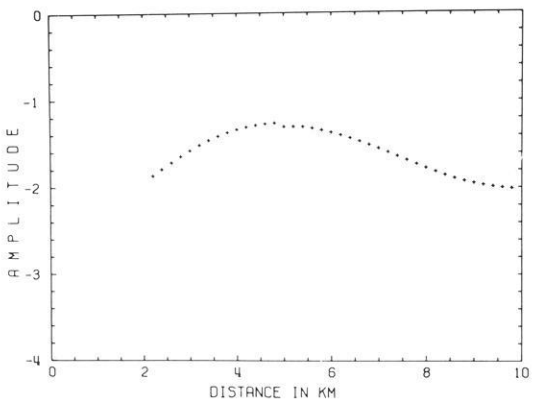

PP REFLECTED WAVE - 4TH INTERFACE

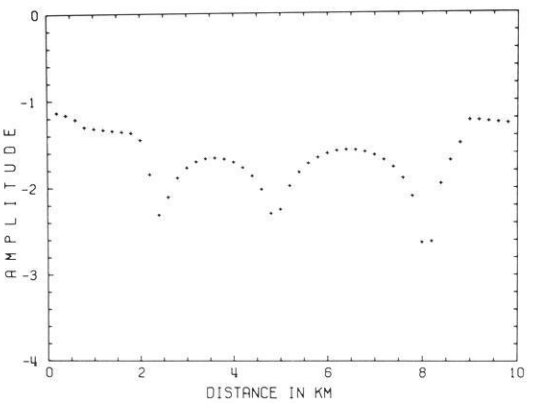

SS REFLECTED WAVE - 5TH INTERFACE

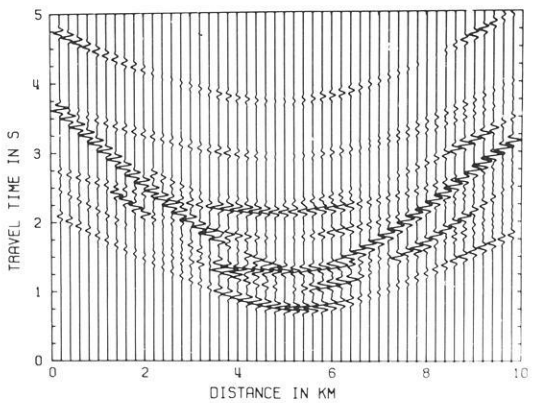

MODEL IP1

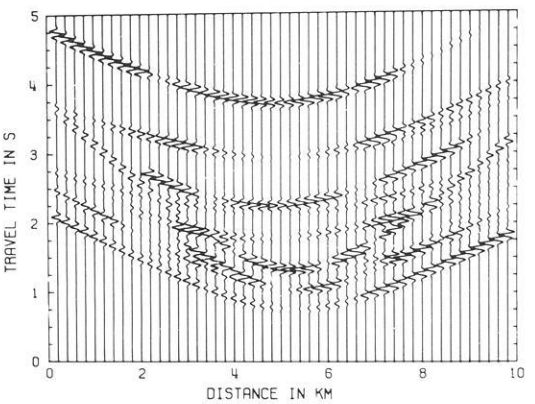

MODEL IP1

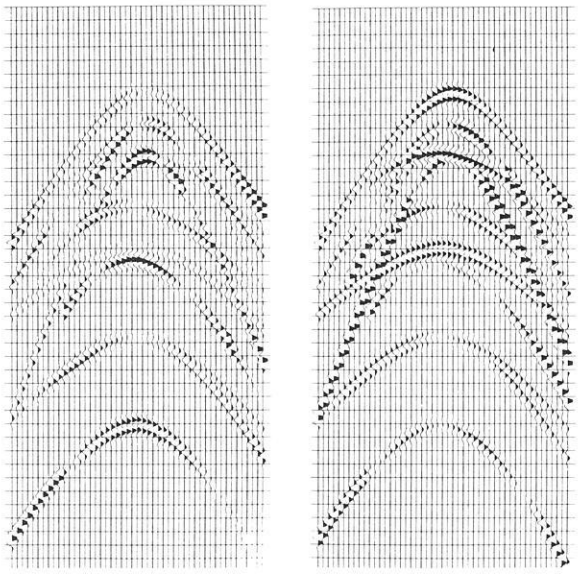

Fig. 4. Model IP1, shot point at $x=5$ km. Ray synthetic seismograms of the vertical component (*left*) and horizontal component (*right*) of the displacement vector. The travel time is not reduced; the time axis is oriented downwards, from 0 s to 5 s. The horizontal axes again correspond to x, from 0 km to 10 km. All primary reflected waves, including converted waves, are considered. A standard seismic plotting system is used to plot the synthetic seismogram sections

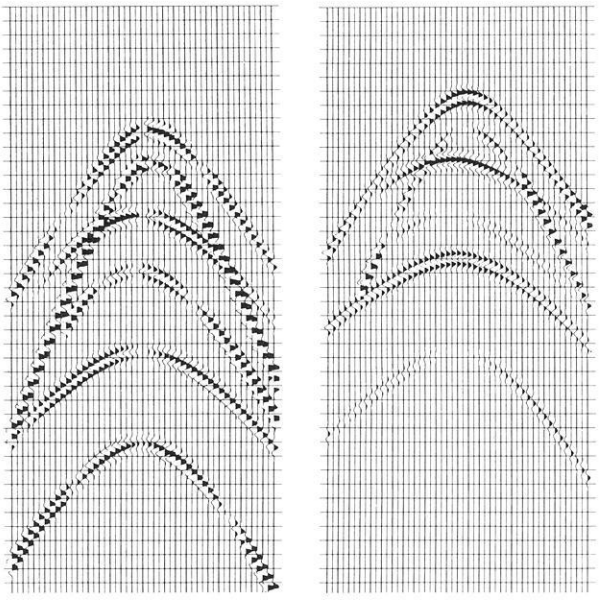

Fig. 5. Model IP1, shot point at $x=5$ km. Ray synthetic seismograms of the vertical component of the displacement vector. *Left-hand side:* The source generates only P waves. *Right-hand side:* The source generates only S waves. Primary reflected waves, including converted waves, are considered. The travel time is not reduced; the time axis is oriented downwards, from 0 s to 5 s. The horizontal axes again correspond to x, from 0 km to 10 km. A standard seismic plotting system is used to plot the synthetic seismogram sections

10. Numerical example 1: model IP1

We shall now illustrate the ray synthetic seismogram computations on a simple 2-D laterally varying model IP1, see Fig. 2. The model is 10 km long and 4.5 km deep. It contains a lens-like high-velocity body. For simplicity, the velocities in the individual layers are constant. The P-wave velocities in the individual layers, from top to bottom, are as follows: 2.5 km/s, 3 km/s, 3.5 km/s (the lens), 3 km/s, 4 km/s. The S-wave velocities V_s and the densities ρ are evaluated from the P-wave velocities V_p using the relations: $V_s=V_p/\sqrt{3}$, $\rho=1.7+0.2\,V_p$. The uppermost interface is curved and represents the Earth's surface. In Fig. 2 the region above the Earth's surface is denoted by asterisks. A point source with isotropic radiation patterns generates both P and S waves, the generated S waves being twice as strong as the P waves.

The synthetic seismograms for the IP1 model were calculated using the SEIS81 program package. We shall briefly describe a revised version of the program package, called SEIS83, which is now available from the World Data Center A for Solid Earth Geophysics, Boulder. A more detailed description of the SEIS83 program package can be found in Červený and Pšenčík (1984).

The *SEIS83 program package* is designed for the numerical modelling of high-frequency seismic wave fields in 2-D laterally varying layered structures by the ray method. It is based on two-point ray tracing. The two-point ray tracing is performed by a modified shooting method. Special care in the modified shooting procedure is devoted to multiple arrivals of the individual elementary waves, to boundaries of shadow zones and to slightly refracted waves.

The model is bounded by two vertical boundaries and two, possibly curved, boundaries representing the Earth's surface and the bottom of the model. Each interface crosses the whole model from its left vertical boundary to its right vertical boundary. The interfaces are specified by systems of points. They are approximated by cubic spline interpolation. They may have corner points and may be fictitious in certain parts. Various interfaces may also partially coincide. Thus, models with vanishing layers, block structures, fractures and isolated bodies can be handled. A slight dissipation is optionally considered. Within any layer, the velocity distribution may be approximated optionally in one of the three following ways:

a) The velocities are specified at grid points of a rectangular network covering the whole layer and a bicubic spline approximation is used.

b) The same as in a), but the piecewise bilinear approximation is used instead of splines.

c) The velocity is specified by isolines of velocity, and a linear velocity-depth interpolation between isolines is used.

The ray synthetic seismograms are evaluated by the summation of elementary seismograms. The source-time

Fig. 6. Model IP1, shot point at $x=0$ km. Examples of source-to-receiver ray diagrams for four elementary reflected waves. The travel times and ray amplitudes for one of these waves is also shown. *Bottom part:* ray synthetic seismograms of the vertical component (*left*) and horizontal component (*right*) of the displacement vector. No amplitude normalization is used. Travel times are not reduced. All primary reflected waves, including converted waves, are considered

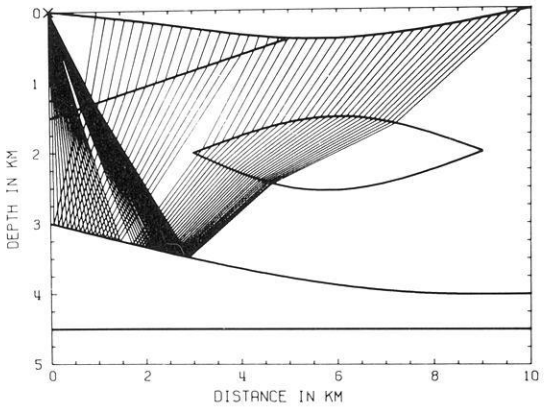

PP REFLECTED WAVE - 5TH INTERFACE

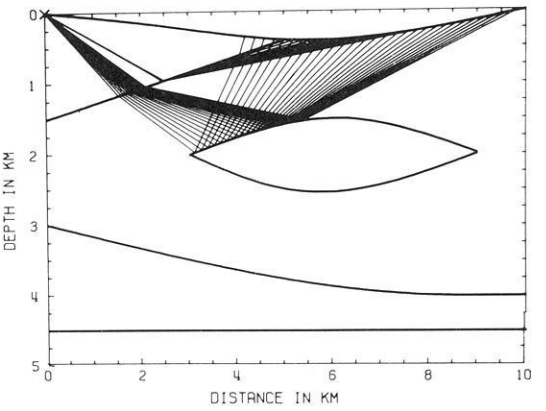

SS-REFLECTED WAVE - 3RD INTERFACE

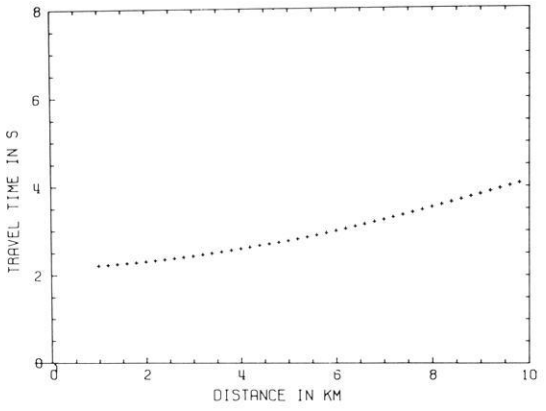

PP REFLECTED WAVE - 5TH INTERFACE

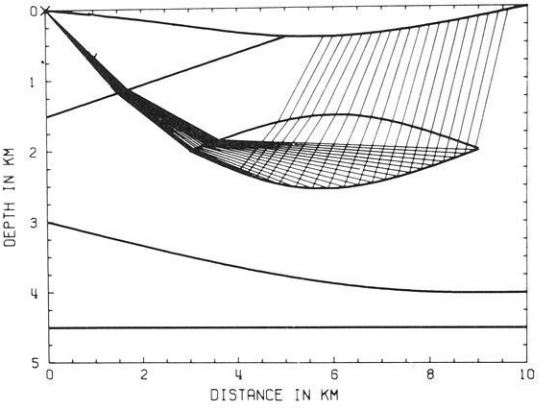

PS REFLECTED WAVE - 4TH INTERFACE

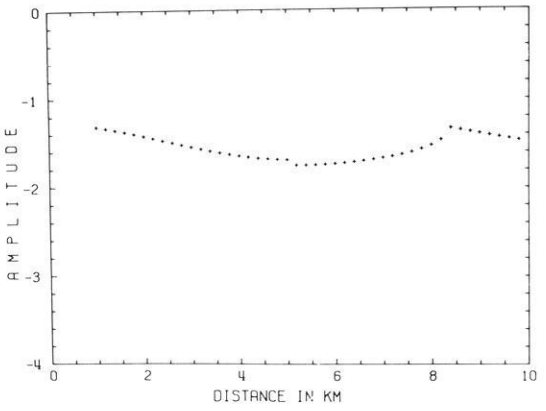

PP REFLECTED WAVE - 5TH INTERFACE

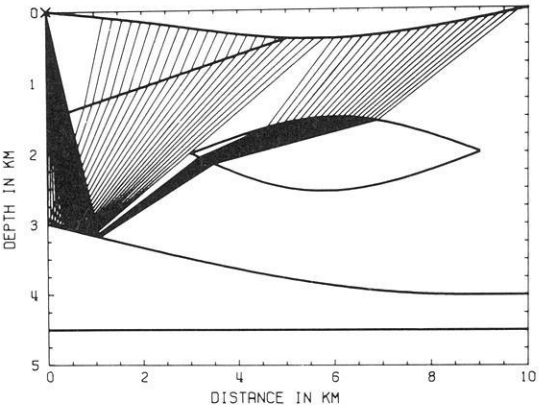

SP REFLECTED WAVE - 5TH INTERFACE

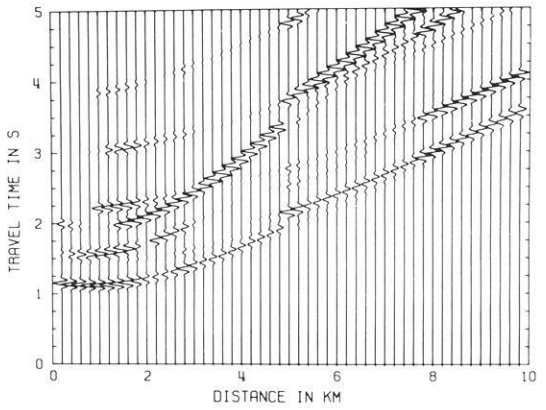

MODEL IP1

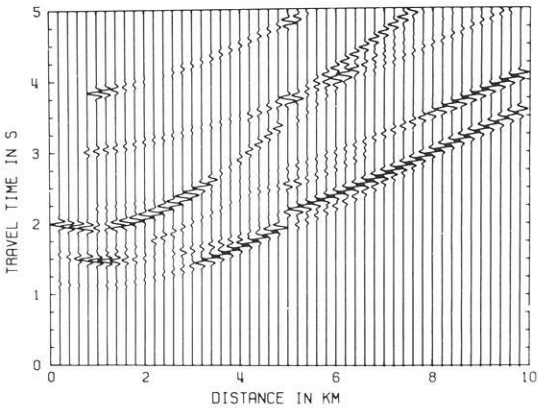

MODEL IP1

function has the form of the Gaussian envelope signal. The source may be situated at any point of the medium. The radiation patterns of the source may be specified independently for P and S waves, either by tables or analytically. The amplitudes are evaluated by standard ray formulae. The geometrical spreading is determined by dynamic ray tracing. The semi-automatic generation of numerical codes of elementary waves is used, see Section 1. All the primary reflected and refracted waves, including the converted waves, may be generated automatically. Any other multiply reflected wave may then be added manually.

Program package SEIS 83 consists of five programs. The basic program, also called SEIS 83, computes two files. The first file contains the elementary wave quantities for all receivers and all elementary waves. The second file contains data for plotting ray diagrams, travel times and amplitudes. The first file may be used to evaluate the synthetic seismograms in the SYNTPL program. These synthetic seismograms may be plotted by program SEISPLOT. The results stored in the second file may be optionally plotted by program RAYPLOT. Program SMOOTH may be optionally used to efficiently prepare the data for the velocity distribution within individual layers and to smooth them. The SEIS 83 program package is well documented.

Now we shall return to our example, model IP1. We shall present results for two different source positions, $x=5$ km and $x=0$ km, situated, in both cases, close to the Earth's surface. A point source with isotropic radiation pattern is considered.

a) Source at $x=5$ km

Figure 3 shows examples of ray diagrams, travel times and amplitudes of two elementary waves: the PP wave reflected from the fourth interface and the SS wave reflected from the fifth interface. (The Earth's surface is considered as the first interface.) Let us emphasize that the ray diagrams are source-to-receiver ray diagrams, not initial-value ones. Note also the considerably more complicated distribution of amplitudes of the SS reflected waves as compared to the amplitudes of the PP reflections. We can also see the distinct boundary of the shadow zone of the reflected PP wave at $x\sim 2$ km. The synthetic seismograms (constructed from PP, PS, SP and SS primary waves reflected from all interfaces) are shown in the bottom part of Fig. 3. Complicated interference zones are clearly seen in both diagrams. It is interesting to observe the focusing of energy at certain epicentral distances, mainly in the case of S waves, in the horizontal component synthetic seismograms.

In Fig. 4, the synthetic seismograms are shown in a different presentation, more common in seismic prospecting, with the time axis oriented downwards. The left-hand synthetic seismograms again correspond to the vertical component, the right-hand to the horizontal component.

It may sometimes be convenient to evaluate only synthetic seismogram sections of some selected elementary waves. As an example, we present Fig. 5. Both synthetic seismogram sections in Fig. 5 correspond to the vertical component. The left-hand picture corresponds to the P-wave source, the right-hand to the S-wave source.

All the computed synthetic seismograms in Figs. 3–5 are presented in terms of actual amplitudes. No reduction of travel times and no amplitude scaling was applied.

b) Source at $x=0$ km

Figure 6 shows examples of several source-to-receiver ray diagrams, travel-time curves, amplitude curves and synthetic seismogram sections for the source situated at $x=0$ km. Note that the elementary wave corresponding to the code of the primary reflected wave from some interface automatically also contains wave refracted in the layer overlying the interface. For demonstration, see the ray diagram of the SS reflected wave. As in the case of the source at $x=5$ km, we can again observe the interesting behaviour of the synthetic seismograms, with many regions of strong arrivals separated by regions of very weak or completely vanishing arrivals.

11. Numerical example 2: model Zurich

In this section, we shall present some results of synthetic seismogram calculations for the 2-D laterally varying Earth's crust model which was used as a "secret model" in the Workshop of the Commission on Controlled Source Seismology at Einsiedeln, 1983, to test various interpretational methods. The model, shown in Fig. 7, was proposed by N.I. Pavlenkova. The Earth's crust consists of two layers. The interfaces are shown by the bold lines in Fig. 7, the thin lines correspond to the isolines of velocity. The dominant feature of the model is an uplift of the deep discontinuities under a sedimentary basin (graben structure). The model is described in detail in the proceedings of the workshop, see Finlayson and Ansorge (1984).

Synthetic seismogram sections were computed for four isotropic shot points, situated at $x=20$ km, 170 km, 320 km and 470 km (six synthetic seismogram sections: 20R, 170L, 170R, 320L, 320R, 470L). All computations were performed using the SEIS 81 program, see Section 10.

In Fig. 8, ray diagrams, travel times and amplitudes for several elementary waves propagating to the right of SP = 320 km are shown. In particular, we can see the P waves refracted in the first, second and third layers and the PP waves reflected from the intermediate interface and from the Mohorovičić discontinuity. The travel time is reduced, the reduction velocity being 8 km/s.

The reflected waves from the intermediate interface and from the Mohorovičić discontinuity are recorded continuously from the shot point at $x=320$ km to $x=500$ km and $x=475$ km, respectively. Beyond these distances, shadow zones are formed. The critical points corresponding to these waves are situated at $x=385$ km and $x=410$ km, respectively. At these distances, the ray amplitudes of the

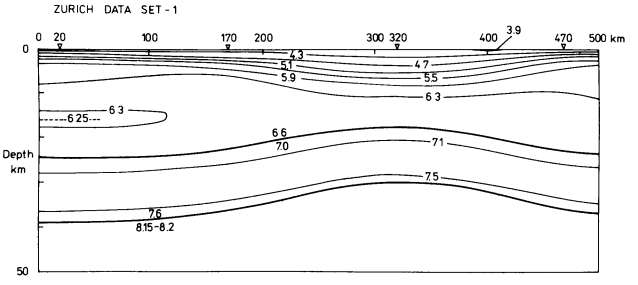

Fig. 7. The 2-D laterally varying Earth's crust model Zurich, used for the computation of numerical example 2. The *bold lines* denote interfaces, the *thin lines* the isolines of velocity. The shot points are situated at $x=20$ km, $x=170$ km, $x=320$ km and $x=470$ km

reflected waves reach their maximum values. The wave refracted in the first layer is recorded continuously from the source to $x=500$ km, the wave refracted in the second layer from $x=385$ km to $x=475$ km and, finally, the wave refracted under the Moho is observed beyond $x=415$ km. Note that the program package SEIS81 did not give quite accurately the identification of the boundaries of shadow zones in certain situations. The program package SEIS83, improved in this respect, gives the boundaries of shadow zones at $x=500$ km and $x=485$ km (not $x=475$ km).

The wave refracted in the first layer has very large amplitudes at small epicentral distances, close to the shot point. In this region, the amplitudes are not quite regular, see Fig. 8. The irregularities are caused by changes of velocity gradients in the source region and by corresponding (slight) oscillations of the depth derivatives of the spline approximation. For the detailed behaviour of the ray field in this region, refer to Červený (1985a, Figs. 15a and 15b).

The synthetic seismogram section for the Zurich model, SP = 320 km, evaluated by the program package SEIS83, is presented in Fig. 9a. The source-time function corresponds to the Gaussian envelope signal, with $f_M=4$ Hz, $\gamma=4$, $t_0=0$ s and $\nu=0$. The zero time of the source-time function corresponds to the maximum of the envelope of the signal, i.e. to the middle of the signal. The reduction velocity is 8 km/s. Amplitude power scaling is used, the trace at the epicentral distance r being multiplied by $35(r/20)^1$. Here, r is measured in kilometres and amplitude = 1 corresponds to the plotting distance between two neighbouring traces in the plot of the seismogram section.

The synthetic seismogram section is considerably different in three ranges of epicentral distances. At small epicentral distances, a strong refracted wave is followed by weak reflections from the intermediate interface and from the Moho. The weak arrivals at a reduced time of about 7.5 s at $x\sim360$–380 km correspond to the primary reflected converted *PS* wave from the intermediate interface. (The primary reflected converted *PS* wave from the Moho is outside the range of travel times under consideration.) Individual waves are well separated from each other. At larger epicentral distances, $r\sim70$–130 km, the individual waves mutually interfere. At large epicentral distances, $r\gtrsim140$ km, the individual waves are again separated to some extent. The very weak refracted wave propagating under the Moho appears in the first arrivals. In the second arrivals, the wave reflected from the Moho appears. The wave interferes with the wave refracted in the deep crust in that region. Finally, the reflected wave from the intermediate interface arrives as the last. Again, this wave interferes with the wave refracted in the first layer. The boundaries of shadow zones for these waves are situated beyond $x=485$ km and $x=500$ km, respectively, as discussed above. As the ray method is used, the boundaries between the illuminated and shadow regions are sharp.

The general behaviour of the synthetic sections for other shot points is similar to that in Fig. 9a. A more complicated synthetic section is obtained for SP = 20 km, due to the low-velocity layer, see Fig. 9b. The refracted wave propagating in the first layer has several branches in this case. The rays of refracted waves which penetrate to the deeper parts of the first layer form a new retrograde branch beyond $x=215$ km, with a short loop and a caustic point close to $x=215$ km. Otherwise, the synthetic section for SP = 20 km is similar to that for SP = 320 km. The wave reflected from the intermediate interface has a critical point at $x\sim125$ km and the boundary of the shadow zone at $x\sim210$ km. The wave reflected from the Moho discontinuity has the same points at $x\sim135$ km and $x\sim215$ km. The wave refracted below the Moho is too weak to be observed in the section.

The synthetic seismograms for the same model and for SP = 320 km, calculated by the Gaussian beam method, are presented in Červený (1985a) in this volume. The differences between the ray synthetic seismograms and Gaussian beam synthetic seismograms are discussed there in some detail. (Note only that the zero time of the source-time function in the Gaussian beam computations is shifted by 0.4 s with respect to ray computations and that $f_M=5$ Hz, not 4 Hz.) The above reference also presents Gaussian beam synthetic seismograms for the same model and the same shot point, assuming various radiation patterns of the source (single force, double couple), and allowing some slight dissipation in the medium.

Similarly, synthetic seismograms for model Zurich, SP = 20 km, evaluated by a 3-D program package as a weighted superposition of paraxial ray approximations from the nearest endpoints of rays are presented in Fig. 13 of this paper. For discussion, see Section 14.

Note that the ray synthetic seismograms for model Zurich and all shot points (SP = 20 km, 170 km, 320 km, 470 km), computed by Červený and Pšenčík, can be found in Finlayson and Ansorge (1984). The publication also presents ray synthetic seismograms for several similar laterally varying 2-D layered crustal models, computed by various authors in the process of interpreting the "secret" model Zurich (V. Luosto, E.R. Flüh and B. Milkereit, C.M.R. Fowler, G.S. Fuis and T.J. Reed, D. Gajewski, B. Guggisberg, N. Sierro, J. Ansorge, M. Demartin and E. Banda, W.D. Mooney). It is obvious from this list that synthetic seismograms are now a widely used tool for the interpretation of deep seismic sounding data. In one paper (by C. Prodehl), the ray synthetic seismograms for SP = 20 km are compared with the reflectivity seismograms for a vertically inhomogeneous (but laterally homogeneous) modification of model Zurich.

12. Numerical example 3: profile Baigezhuang-Fengning

The next example is taken from actual deep seismic sounding measurements of the Earth's crust in China. In interpreting the measured data, numerical modelling has been used. In the numerical modelling, the synthetic seismogram sections for models based on a preliminary kinematic interpretation were computed. We shall present one synthetic seismogram section from the Baigezhuang-Fengning profile, SP = 112 km. Note that the profile passes in the close vicinity of the city of Tangshan, well-known for the catastrophic 1976 earthquake. The preliminary model used for the computation is as follows. The crust consists of four layers and the average depth of the Moho is 34 km. The interfaces are roughly horizontal, but the velocity in the individual layers changes considerably both in the horizontal and vertical directions. Indications of several low-velocity regions were found. To be brief we shall not present the measured seismogram sections and a detailed description of the proposed model. The synthetic seismograms for SP = 112 km are shown in Fig. 10. They were computed by the program package SEIS83. The reduction velocity

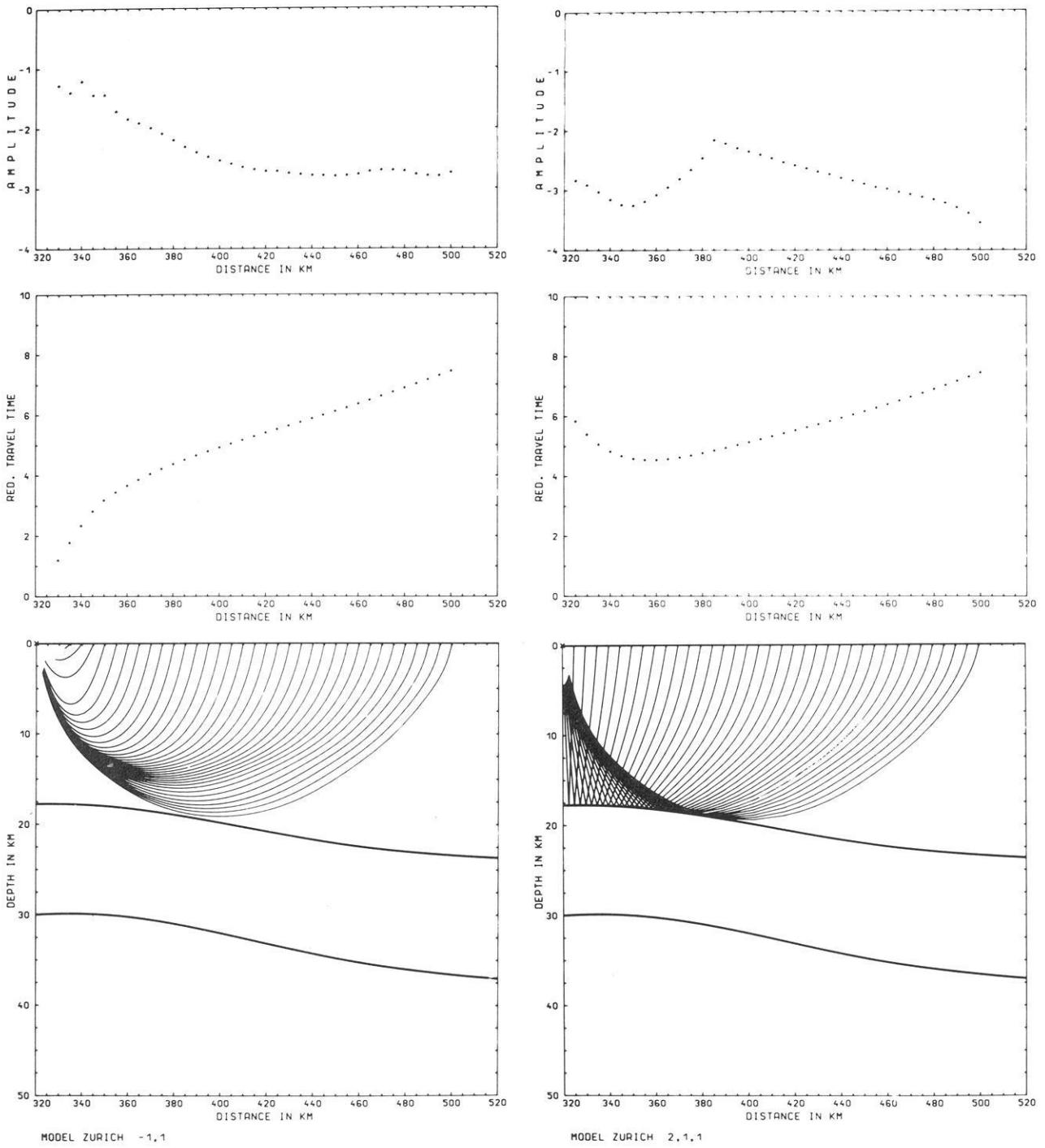

Fig. 8. Model Zurich, shot point at $x=320$ km. Examples of source-to-receiver ray diagrams, travel-time and amplitude-distance plots for elementary reflected and refracted P waves

is 6 km/s. The Gaussian envelope signal with $f_M=4$ Hz, $\gamma=4$, $\nu=0$, $t_0=0$ s was used in the computations as the source-time function.

The most interesting feature in Fig. 10 is the complicated behaviour of the amplitudes of the Pg waves which are the first arrivals to both sides of the shot point. The amplitudes of seismic waves are more sensitive to anomalies in the velocity distribution than the travel times. We can also see that the properties of the waves reflected from intermediate crustal interfaces change considerably in the lateral direction. The last arrival is the Moho reflection.

13. Numerical example 4: salt dome model

In this section, we shall present an example of the computation of synthetic time sections. The synthetic time sections were computed using the SYNS83 program package which is based on the normal ray algorithm. The SYNS83 program package is a modification of the SEIS83 package. The approximation of the velocity distribution in the model is the same as in SEIS83. The main difference between SEIS83 and SYNS83 is that the rays normal to individual reflecting interfaces are evaluated in SYNS83. In this way,

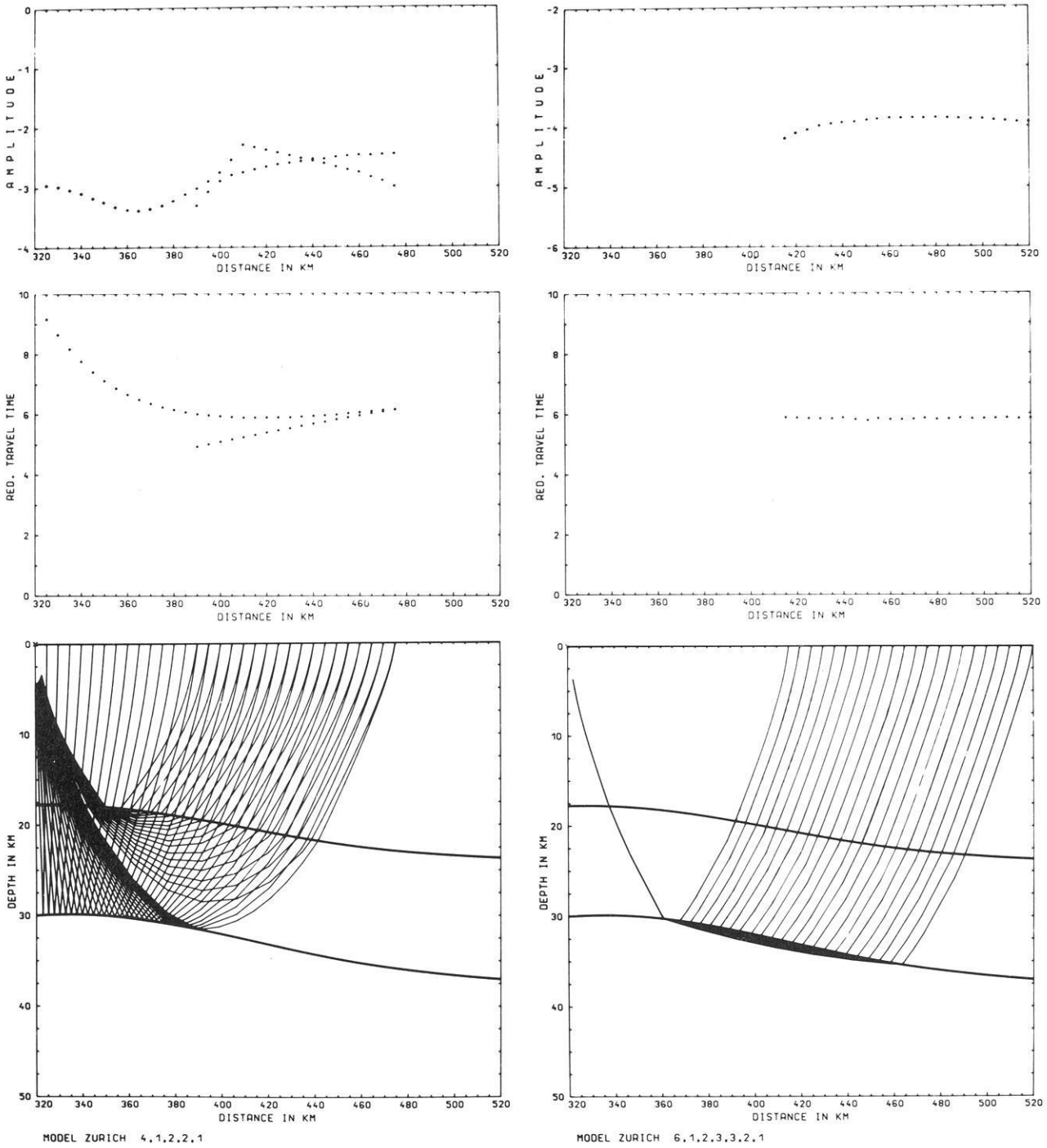

the ray parameter does not correspond to the radiation angle from the source, but the x-coordinate along the normally reflecting interface under consideration. Boundary-value ray tracing is used to evaluate the normal rays arriving at receivers. Most of the other details are the same as in SEIS83.

Synthetic time sections were computed for the salt dome model, see Fig. 11. The model was proposed by J. Fertig. It consists of six layers, separated by five interfaces. The interfaces partially coincide and partially vanish. The velocity is constant within the individual layers. The resulting synthetic time sections are shown in Fig. 11, both for the vertical component (above) and horizontal component (below). The synthetic time sections are normalized. Again, the Gaussian envelope signal is considered, with $\gamma=4$, $f_M=10$ Hz, $\nu=0$, $t_0=0$ s.

Figure 12 shows normal ray diagrams for elementary waves corresponding to the second, third, fourth and fifth interfaces, and the normal two-way travel times and vertical amplitudes for the second interface. The diagrams are self-explanatory. As we can see, certain anomalies are caused by the corners of the interfaces, mainly by the corners of

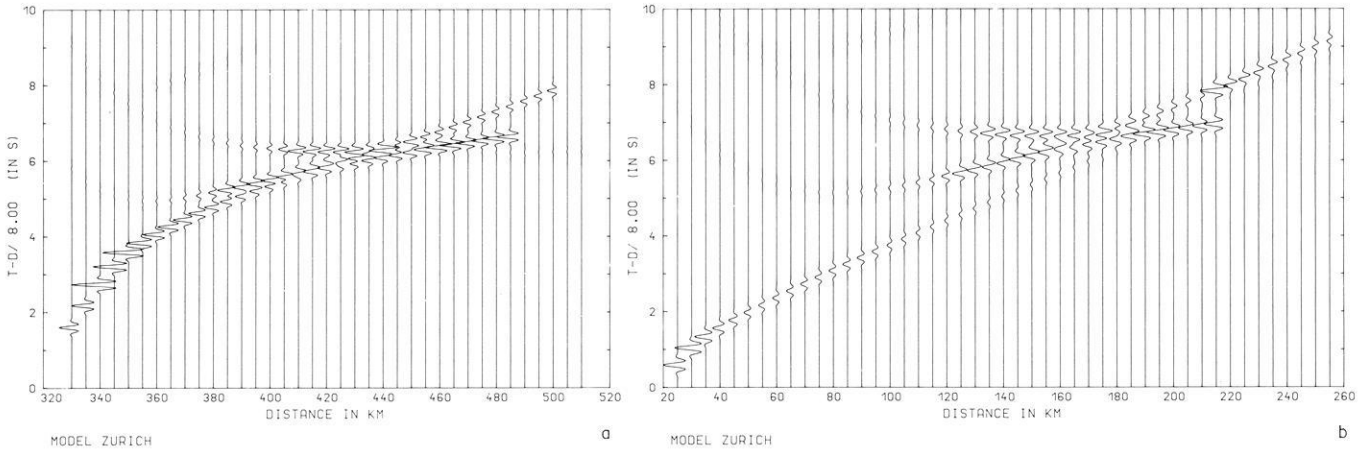

Fig. 9a and b. Model Zurich. Ray synthetic seismograms of the vertical component of the displacement vector. Only primary reflected *PP* and *PS* and refracted *P* waves are considered. The travel-time axis is reduced, the reduction velocity being 8 km/s. Power scaling of amplitudes with the epicentral distance is used. **a**: Shot point SP = 320 km. **b**: Shot point SP = 20 km

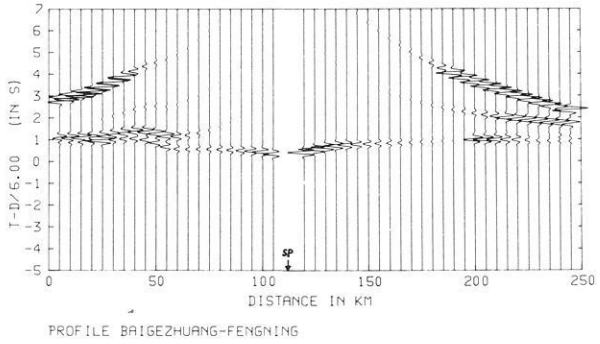

Fig. 10. Ray synthetic seismograms of the vertical component of the displacement vector along the Baigezhuang-Fengning profile

the second interface. In the relevant regions, the ray method is not too suitable for computations. It would be useful to also evaluate, in addition to the standard ray contributions, the edge waves connected with these corners, see Klem-Musatov and Aizenberg (1984). Another possibility is to smooth the interface or to use Gaussian beams.

It is, however, obvious from the diagrams presented that the ray computations may be useful in the interpretation even without the modifications mentioned above.

In the example presented, we have considered the model with constant velocities in the individual layers. The SYNS83 program package allows an arbitrary velocity distribution to be considered in any layer, as in SEIS83.

14. Numerical example 5. 3-D computations by weighting of the paraxial ray approximations

In this section, we shall present one example of computing synthetic seismograms by the program package SW84, designed for 3-D numerical modelling of seismic wave fields in complex structures (Klimeš 1985). The synthetic seismograms which will be presented here are computed as a weighted superposition of paraxial ray approximations from the nearest endpoints of rays.

The *SW84 program package* is composed of a system of optional programs and routines. The routines for evaluating the interfaces and velocity distributions in the individual layers may be specified by the user. Certain standard options, based on splines with tension, are included in the package. The generation of numerical codes of elementary waves is manual, but the numerical codes are constructed in such a way that one code may include several elementary waves. Cauchy initial-value ray tracing is performed. The increments in the radiation angles from the source, however, are not necessarily constant but they are optionally controlled in such a way as to obtain the required density of endpoints of rays in region D_0 of interest along the Earth's surface. Thus, some sort of interval ray tracing is used. The point source may be situated at any point of the model. It may generate both *P* and *S* waves. In the older version of the program package, called RD83 (see Červený et al. 1984), the synthetic seismograms were evaluated by the summation of elementary seismograms, corresponding to the Gaussian envelope source-time function (as in SEIS83). In SW84, the frequency-domain approach is implemented, which allows the use of an arbitrary high-frequency source-time function. The fast frequency response (FFR) algorithm, described in Section 8, is used. The radiation patterns correspond to an isotropic, single-force or to a general moment-tensor source. Slight dissipation may be considered.

The program package SW84 works in two different modes:

1) *Complete 3-D mode.* This mode is suitable for completely 3-D calculations of synthetic seismograms. This is the case of receivers distributed regularly or irregularly along some region D_0 of interest along the Earth's surface. In this mode, a two-parametric system of rays is evaluated. Both the radiation angles δ_0 and φ_0 from the source vary in broad limits to cover the whole region D_0 with endpoints of rays.

2) *Profile mode.* This mode is suitable for computations of synthetic seismograms at receivers situated roughly along a straight-line profile, if the epicentre is located close to the profile. In this mode, only a one-parametric system of rays, with the initial directions in some vertical plane containing the source, is evaluated. From the two radiation

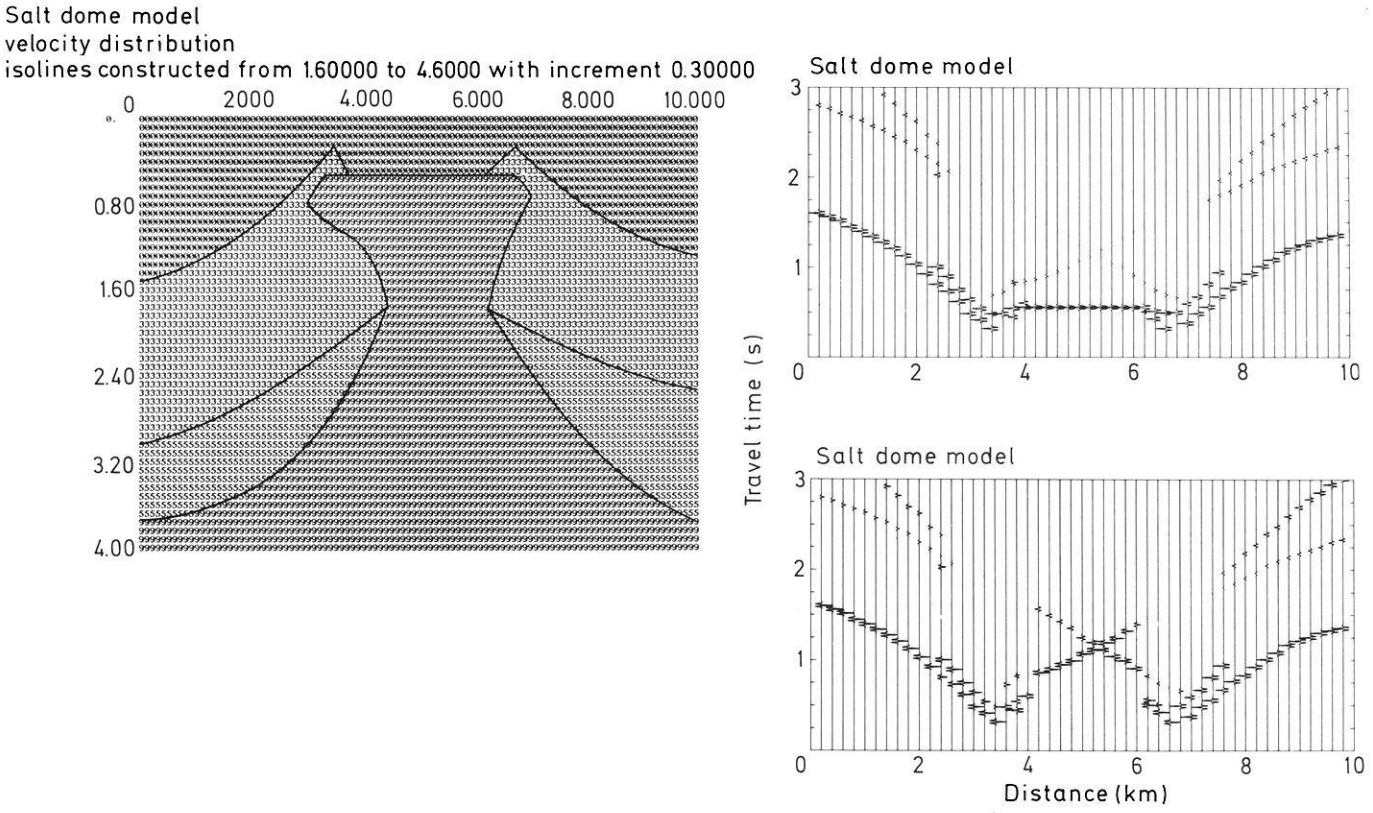

Fig. 11. Synthetic time sections for the salt dome model. *Left-hand side:* Model. The velocities in the individual layers are constant. *Right-hand side:* Synthetic time sections for the vertical (*top*) and horizontal (*bottom*) components of the displacement vector. Normalized amplitudes

angles δ_0 and φ_0, only one (say δ_0) is changed, and the second (φ_0) remains fixed. As the model is three-dimensional, the endpoints of rays are not generally situated in that vertical plane. The methods of paraxial ray approximation allow us to evaluate approximately the wave field at receivers situated in the vicinity of endpoints of rays. The standard paraxial approximation is used in the direction of the coordinate line corresponding to the ray coordinate φ_0, going through the endpoint. In the plane perpendicular to that coordinate line, Gaussian weighting of paraxial ray approximations is used. In the profile mode of the program package SW84, the receivers are generally chosen along a straight-line profile or along a slalom-line profile on the Earth's surface. The most accurate results are obtained if the profile roughly follows the endpoints of rays. In 3-D models, which are not strongly inhomogeneous in the direction perpendicular to the vertical plane discussed above, the position of the profile is not so critical. For example, the profile may follow the intersection of the Earth's surface with the vertical plane.

Note that ray tracing, dynamic ray tracing, etc., is fully three-dimensional in both modes. The profile mode, however, is considerably faster, as only a one-parametric system of rays is evaluated. It does not require a considerably longer computer time than 2-D computations.

Once a file with elementary wave quantities at the endpoints of rays is available, it may also be used for Gaussian beam computations. In this way, the program package SW84 may even be used for the evaluation of Gaussian beam synthetic seismograms, see Červený (1985a). The Gaussian weighting of paraxial ray approximations corresponds, in principle, to the summation of very narrow Gaussian beams, with their phasefronts at the endpoints of rays locally identical to the wavefronts of elementary waves under consideration at the same point. See the relevant equations in Červený [1985a, Eq. (18)]. The width of the Gaussian window is selected automatically to be as narrow as possible. The lower limit of the width is controlled by the local density of the endpoints of rays.

We shall now present one examle of computations, again for model Zurich, as we would like to compare the 3-D paraxial ray approximation computations with the 2-D two-point ray-tracing computations, see Section 11. Although the model is two-dimensional, all the computations are three-dimensional.

Figure 13 shows synthetic seismograms for model Zurich, SP = 20 km, evaluated by Gaussian weighting of paraxial ray approximations. The profile mode is used for computations. From the interpretational point of view, Fig. 13 and Fig. 9b are very similar. The only difference is that the weighting of paraxial ray approximations (Fig. 13) involves some smoothing. In this way, the boundaries of shadow zones and critical regions are not as sharp as in Fig. 9b, but slightly smoothed. Similarly, the caustic region close to $x = 215$ km is smoothed. The reflections from the intermediate interface and the retrograde branch of the refracted wave are all smoothly connected at $x \sim 205$–215 km, so that they apparently form one wave.

It should be noted that the smoothing effect introduced by the Gaussian weighting of paraxial ray approximations

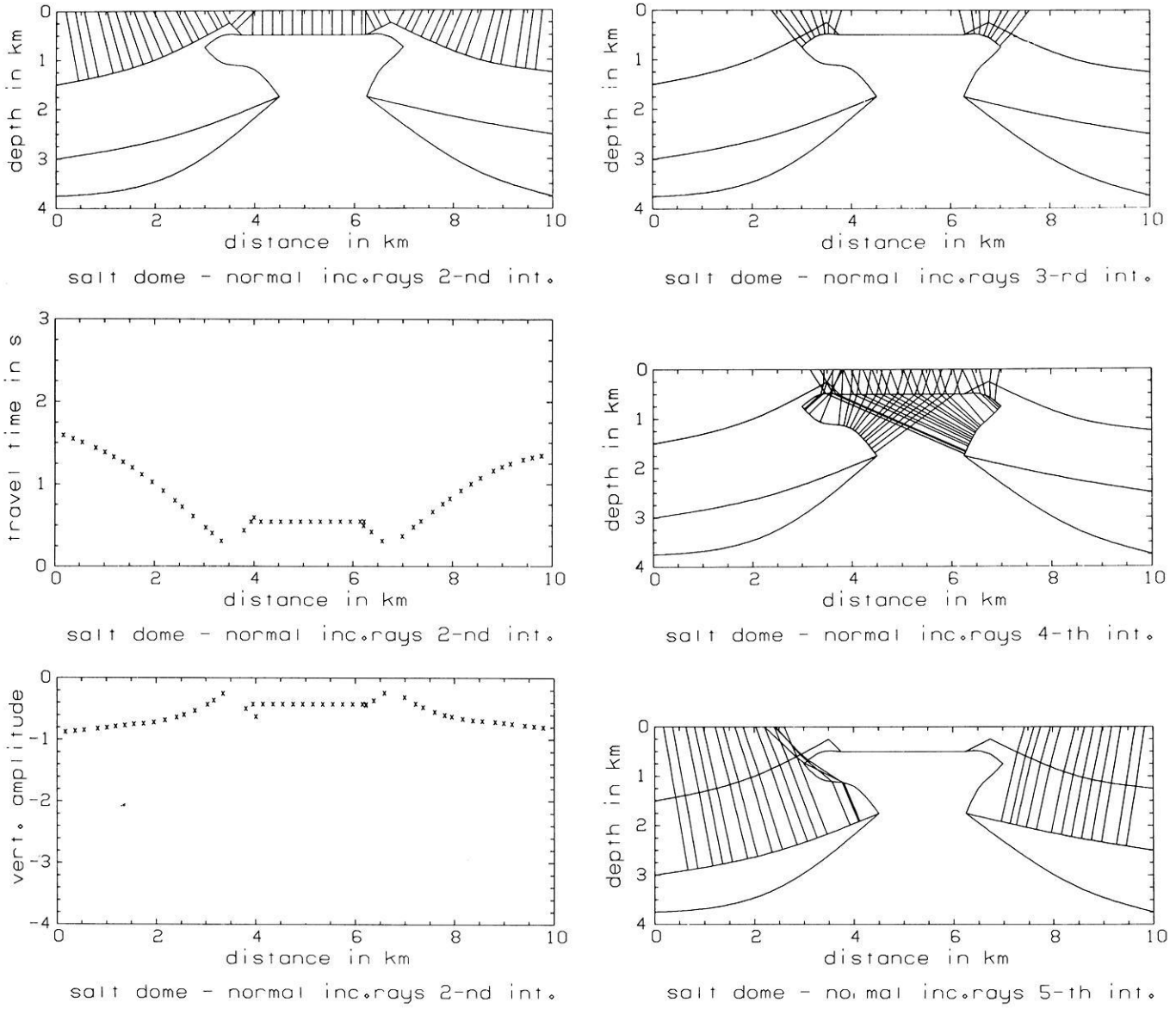

Fig. 12. Salt dome model. Exampoles of normal ray diagrams for several elementary waves. The normal two-way travel times and ray amplitudes for one of these elementary waves are also shown

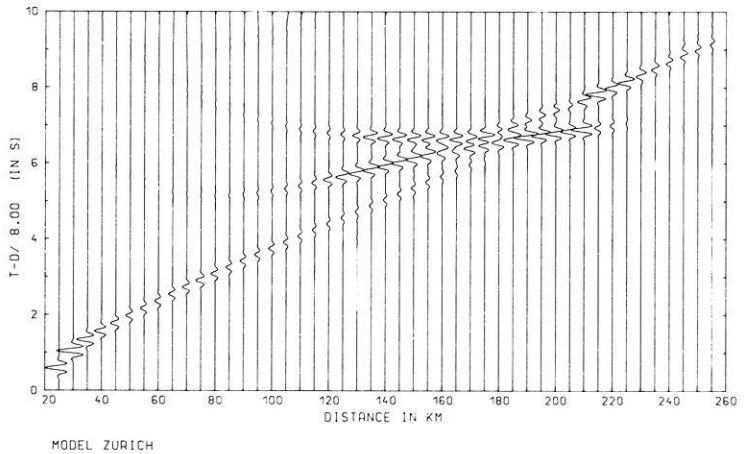

Fig. 13. 3-D computations. Model Zurich, shot point at $x = 20$ km. Ray synthetic seismograms of the vertical component of the displacement vector, evaluated as weighted superposition of paraxial ray approximations. Compare with Fig. 9b

corrects the ray amplitudes in singular regions in a qualitatively correct way. The ray synthetic seismograms computed in this way are, as a rule, closer to exact solutions than the standard two-point ray tracing solutions. Quantitatively, however, the results in singular regions may still be rather different from the exact solutions. In the terminology of Gaussian beams, very narrow Gaussian beams are used, whereas broader Gaussian beams are needed in some singular regions to achieve a higher accuracy of the computations.

As a narrow Gaussian window is used in the procedure, the computations of synthetic seismograms based on the weighted summation of paraxial ray approximations is very fast, stable and computationally efficient.

15. Concluding remarks

The ray algorithms and program packages described above can be used, directly or after some modifications, in many other fields of seismology and seismic prospecting. Here we shall list some of them:

a) Strong motion seismogram computations and seismic source mechanism studies. See Bernard and Madariaga (1984), Spudich and Frazer (1984), Madariaga (1985).

b) Effects of structure geometry and local geological conditions on strong ground motion. See Hong and Helmberger (1978), Langston and Lee (1983), Lee and Langston (1983a, b).

c) Polarization studies (mainly for S waves). See Cormier (1984).

d) Location of seismic hypocentres. Location of rockbursts in mines. See Lee and Stewart (1981), Engdahl (1984).

e) Solution of inverse problems for laterally varying media. Seismic tomography. References are too numerous to given here.

f) Vertical seismic profiling, both in 2-D and 3-D models. See Cormier and Mellen (1984), Young et al. (1983), Sierra Geophysics (n.d.).

g) Seismic migration. See, e.g., Hubral and Krey (1980), Zilkha et al. (1983), and other references given there.

h) Determination of interval velocities and curvatures of reflecting interfaces in reflection seismology. See Hubral and Krey (1980).

i) True (spreading-free) amplitude determination in reflection seismology. See Hubral (1983).

j) Backward and forward continuation of the wave field specified on an initial surface of arbitrary form. See Červený (1985b).

k) Borehole-to-borehole measurements.

The above list is, of course, far from complete. The number of applications of the ray method in seismology and seismic prospecting of complex media continuously increases.

Acknowledgements. The author is greatly indebted to Ivan Pšenčík and Luděk Klimeš for everyday discussions of the problem of high-frequency seismic wave propagation in complex laterally varying structures. He is also greatly indebted to the Stanford Exploration Project and personally to its Director, Prof. Jon Claerbout, who invited the author and Ivan Pšenčík to work at the Department of Geophysics of the Stanford University for several months. During these stays, the SEIS81, SEIS83 and SYNS83 program packages were improved and modified considerably, and numerical Examples 1 and 4, presented in this paper, were computed (Example 4 by I. Pšenčík). Numerical Example 3 was computed during the author's stay with the Geophysical Prospecting Brigade, State Seismological Bureau at Zhengzhou, China. The author wishes to express his sincere thanks to the Chinese colleagues (especially to Dr. Sun Wucheng and Dr. Liu Changquan) for useful discussions of and comments on the problem of numerical modelling of seismic wave fields in complex structures.

References

Achenbach, J.D.: Wave propagation in elastic solids. Amsterdam: Elsevier 1973

Aki, K., Richards, P.: Quantitative seismology. San Francisco: Freeman 1980

Alekseyev, A.S., Gel'chinskiy, B.Ya.: On the ray method of computation of wave fields for inhomogeneous media with curved interfaces. In: Problems of the dynamic theory of propagation of seismic waves (in Russian), Vol. 3, G.I. Petrashen, ed. pp. 107–160. Leningrad: Leningrad Univ. Press 1959

Aric, K., Gutdeutsch, R., Sailer, A.: Computation of travel times and rays in a medium of two-dimensional velocity distribution. Pageoph. **118**, 796–806, 1980

Azbel, I.Y., Dmitrieva, L.A., Yanovskaya, T.B.: The technique for calculation of geometrical spreading in three-dimensional media. In: Computational seismology (in Russian), Vol. 13, V.I. Keilis-Borok, A.L. Levshin, eds.: pp. 113–127. Moscow: Nauka 1980

Babich, V.M.: Ray method of the computation of the intensity of wave fronts (in Russian). Doklady Akad. Nauk SSSR **110**, 355–357, 1956

Babich, V.M.: Ray method of the computation of the intensity of wave fronts in elastic inhomogeneous anisotropic medium. In: Problems of the dynamic theory of propagation of seismic waves (in Russian), Vol. 5, G.I. Petrashen, ed.: pp. 36–46. Leningrad: Leningrad Univ. Press 1961

Babich, V.M.: On the space-time ray method in the theory of elastic waves (in Russian). Izv. Akad. Nauk SSSR, Fizika Zemli No. 2, 3–12, 1979

Babich, V.M., Alekseyev, A.S.: On the ray method of the computation of the intensity of wave fronts (in Russian). Izv. Akad. Nauk SSSR, Geophys. Series No. **1**, 9–15, 1958

Babich, V.M., Buldyrev, N.J.: Asymptotic methods in problems of diffraction of short waves (in Russian). Moscow: Nauka 1972

Babich, V.M., Buldyrev, N.J., Molotkov, I.A.: Space-time ray method. Linear and non-linear waves. Leningrad: Leningrad Univ. Press 1985

Ben-Menahem, A., Beydoun, W.B.: Range of validity of seismic ray and beam method in general inhomogeneous media. Part I: General theory. Geophys. J.R. Astron. Soc., 1985a (in press)

Ben-Menahem, A., Beydoun, W.B.: Range of validity of seismic ray and beam method in general inhomogeneous media. Part II: A canonical problem. Geophys. J.R. Astron. Soc., 1985b (in press)

Belonosova, A.V., Cecocho, V.A.: Computation of geometrical spreading in Cartesian coordinates. In: Mathematical methods of the interpretation of geophysical observations (in Russian), A.S. Alekseyev, ed.: pp. 5–11. Novosibirsk: Acad. Sci. USSR, Computing Center 1979

Belonosova, A.V., Tadzhimukhamedova, S.S., Alekseyev, A.S.: Computation of travel-time curves and geometrical spreading in inhomogeneous media. In: Certain methods and algorithms in the interpretation of geophysical data (in Russian), A.S. Alekseyev, ed.: pp. 124–136. Moscow: Nauka 1967

Bernard, P., Madariaga, R.: A new asymptotic method for the modeling of near-field accelerograms. Bull. Seismol. Soc. Am. **74**, 539–557, 1984

Cassel, B.R.: A method for calculating synthetic seismograms in laterally varying media. Geophys. J.R. Astron. Soc. **69**, 339–354, 1982

Červený, V.: Seismic rays and ray intensities in inhomogeneous anisotropic media. Geophys. J.R. Astron. Soc. **29**, 1–13, 1972

Červený, V.: Approximate expressions for the Hilbert transform of a certain class of functions and their applications in the ray theory of seismic waves. Stud. Geophys. Geod. **20**, 125–132, 1976a

Červený, V.: Ray amplitudes in a three-dimensional inhomogeneous medium. Stud. Geophys. Geod. **20**, 401–404, 1976b

Červený, V.: Ray theoretical seismograms for laterally varying structures. J. Geophys. **46**, 335–342, 1979

Červený, V.: Seismic wave fields in structurally complicated media. Ray and Gaussian beam approaches. Lecture notes. Utrecht: Rijksuniversiteit Utrecht, Vening-Meinesz Laboratory 1981a

Červený, V.: Dynamic ray tracing in 2-D media (pp. 21–30). Determination of second derivatives of travel-time fields by dynamic ray tracing (pp. 31–38). Ray tracing in a vicinity of a central ray (pp. 39–48). Computation of geometrical spreading by dynamic ray tracing (pp. 49–60). Dynamic ray tracing across curved interfaces (pp. 61–73). In: Stanford Exploration Project, Rep. No. 28, J. Claerbout, ed. Stanford: Stanford Univ., Dept. of Geophysics 1981b

Červený, V.: Computation of synthetic seismograms for 1-D and 2-D inhomogeneous media. In: Numerical methods in seismic investigations (in Russian), A.S. Alekseyev, ed.: pp. 41–53. Novosibirsk: Nauka 1983

Červený, V.: Gaussian beam synthetic seismograms. J. Geophys. **58**, 44–72 1985a

Červený, V.: The application of ray tracing to the numerical modeling of seismic wavefields in complex structures. In: Handbook of geophysical exploration, Section I: Seismic exploration, K. Helbig and S. Treitel, eds., volume on Seismic shear waves, G. Dohr, ed.: pp. 1–124. London: Geophysical Press 1985b (in press)

Červený, V., Firbas, P.: Numerical modelling and inversion of travel times of seismic body waves in inhomogeneous anisotropic media. Geophys. J.R. Astron. Soc. **76**, 41–51, 1984

Červený, V., Hron, F.: The ray series method and dynamic ray tracing systems for 3-D inhomogeneous media. Bull. Seismol. Soc. Am. **70**, 47–77, 1980

Červený, V., Janský, J.: Fast computation of ray synthetic seismograms in vertically inhomogeneous media. Stud. Geophys. Geod. **29**, 49–67, 1985

Červený, V., Novák, B.: Theoretical seismograms in the Earth's crust composed of homogeneous layers. Program S1 (in Czech). Research Report No. 5. Prague: Charles Univ., Inst. of Geophysics 1968

Červený, V., Pšenčík, I.: Ray theoretical seismograms for laterally varying layered structures. In: Publ. Inst. Pol. Acad. Sci., A-4 (115): pp. 173–185, Warszawa-Lodz: PWN 1977

Červený, V., Pšenčík, I.: Ray amplitudes of seismic body waves in laterally inhomogeneous media. Geophys. J.R. Astron. Soc. **57**, 97–106, 1979

Červený, V., Pšenčík, I.: Gaussian beam and paraxial ray approximation in three-dimensional elastic inhomogeneous media. J. Geophys. **53**, 1–15, 1983

Červený, V., Pšenčík, I.: SEIS83-Numerical modeling of seismic wave fields in 2-D laterally varying layered structures by the ray method. In: Documentation of Earthquake Algorithms, Report SE-35, E.R. Engdahl, ed.: pp. 36–40. Boulder: World Data Center (A) for Solid Earth Geophysics 1984

Červený, V., Ravindra, R.: Theory of seismic head waves. Toronto: Univ. of Toronto Press 1971

Červený, V., Fuchs, K., Müller, G., Zahradník, J.: Theoretical seismograms for inhomogeneous media. In: Problems of the dynamic theory of propagation of seismic waves (in Russian), Vol. 20, G.I. Petrashen, ed.: pp. 84–109. Leningrad: Nauka 1980

Červený, V., Klimeš, L, Pšenčík, I.: Paraxial ray approximations in the computation of seismic wavefields in inhomogeneous media. Geophys. J.R. Astron. Soc. **79**, 89–104, 1984

Červený, V., Langer, J., Pšenčík, I.: Computation of geometrical spreading of seismic body waves in laterally inhomogeneous media with curved interfaces. Geophys. J.R. Astron. Soc. **38**, 9–19, 1974

Červený, V., Molotkov, I.A., Pšenčík, I.: Ray method in seismology. Praha: Karlova Universita 1977

Červený, V., Molotkov, I.A., Pšenčík, I.: Space-time ray method for seismic ray fields. Stud. Geophys. Geod. **26**, 342–351, 1982

Chander, R.: On tracing seismic rays with specified end points. J. Geophys. **41**, 173–177, 1975

Chapman, C.H.: Ray theory and its extensions – WKBJ and Maslov seismograms. J. Geophys. **58**, 27–43, 1985

Chiang, C.S., Braile, L.W.: An example of two-dimensional synthetic seismogram modelling. Bull. Seismol. Soc. Am. **74**, 509–520, 1984

Comer, R.P.: Rapid seismic ray tracing in a spherically symmetric Earth via interpolation of rays. Bull. Seismol. Soc. Am. **74**, 479–492, 1984

Cormier, V.: The polarization of *S* waves in a heterogeneous isotropic Earth model. J. Geophys. **56**, 20–23, 1984

Cormier, V.F., Mellen, M.H.: Application of asymptotic ray theory to vertical seismic profiling. In: Vertical seismic profiling: Advanced concepts, M.N. Toksöz, R.R. Stewart, eds.: pp. 28–44. London: Geophysical Press 1984

Daley, P.F., Hron, F.: Ray-reflectivity method for *SH*-waves in stacks of thin and thick layers. Geophys. J.R. Astron. Soc. **69**, 527–535, 1982

Deschamps, G.A.: Ray techniques in electromagnetics. Proc. IEEE **60**, 1022–1035, 1972

DeSisto, J.A. Smith, R.B.: Comparison of synthetic seismograms. Technical Progress Report. Salt Lake City: University of Utah, Dept. of Geology and Geophysics 1983

Dobrovol'skiy, I.P., Fridman, V.N.: Method of Richardson extrapolation in the ray problem of propagation of seismic waves (in Russian). Izv. Akad. Nauk SSSR, Fizika Zemli No. 3, 42–47, 1980

Engdahl, E.R. (ed.): Documentation of earthquake algorithms, Report SE-35. Boulder: World Data Center (A) for Solid Earth Geophysics 1984

Felsen, L.B., Marcuvitz, N.: Radiation and scattering of waves. Englewood Cliffs: Prentice Hall 1973

Fertig, J., Pšenčík, I.: Numerical modeling of *P* and *S* waves in explosion seismology. In: Handbook of geophysical exploration, Section I: Seismic exploration, K. Helbig and S. Treitel, eds., volume on Seismic shear waves, G. Dohr, ed. London: Geophysical Press 1985 (in press)

Finlayson, D.M., Ansorge, J. (eds.): Workshop proceedings: Interpretation of seismic wave propagation in laterally heterogeneous structures. Report 258. Canberra: Bureau of Mineral Resources, Geology and Geophysics 1984

Fridman, V.N.: Numerical-analytical method of the solution of the ray problem. In: Numerical methods in seismic investigations (in Russian), A.S. Alekseyev, ed.: pp. 26–32. Novosibirsk: Nauka 1983

Gebrande, H.: A seismic ray-tracing method for two-dimensional inhomogeneous media. In: Explosion seismology in Central Europe: Data and results. P. Giese, C. Prodehl and A. Stein, eds.: pp. 162–167. Berlin: Springer Verlag 1976

Gel'chinskiy, B.Y.: An expression for the geometrical spreading. In: Problems of the dynamic theory of propagation of seismic waves (in Russian), Vol. 5, G.I. Petrashen, ed.: pp. 47–53. Leningrad: Leningrad Univ. Press 1961

Gerasimenko, A.N.: Ray method in geometrical seismics of structurally complex layered media (in Russian). Kiev: Naukovaya Dumka 1982

Gjoystdal, H., Reinhardsen, J.E., Ursin, B.: Travel-time and wavefront curvature calculations in inhomogeneous layered media with curved interfaces. Geophysics **49**, 1466–1494, 1984

Goldin, S.V.: Interpretation of seismic reflection data (in Russian). Moscow: Nedra 1979 (English translation by Tulsa: SEG 1986)

Green, A.G.: Ray paths and relative intensities in one- and two-

dimensional velocity models. Bull. Seismol. Soc. Am. **66**, 1581–1607, 1976

Grinfeld, M.A.: A new system of equations for calculation of geometrical spreading. In: Computational seismology (in Russian), Vol. 13, V.I. Keilis-Borok, A.L. Levshin, eds.: pp. 127–133. Moscow: Nauka 1980

Hanyga, A.: Dynamic ray tracing in an anisotropic medium. Tectonophysics **90**, 243–251, 1982

Hong, T.L., Helmberger, D.V.: Glorified optics and wave propagation in nonplanar structure. Bull. Seismol. Soc. Am. **68**, 1313–1330, 1978

Hron, F.: Numerical methods of ray generation in multilayered media. In: Methods of computational physics, Vol. 12, B. Bolt, ed.: pp. 1–34. New York: Academic Press 1972

Hron, F., Kanasewich, E.R.: Synthetic seismograms for deep seismic sounding studies using asymptotic ray theory. Bull. Seismol. Soc. Am. **61**, 1169–1200, 1971

Hron, F., Daley, P.F, Marks, L.W.: Numerical modelling of seismic body waves in oil exploration and crustal seismology. In: Computing methods in geophysical mechanics, R.P. Shaw, ed.: pp. 21–42. New York: American Soc. of Mechanical Engineers 1977

Hubral, P.: A wave front curvature approach to the computing of ray amplitudes in inhomogeneous media with curved interfaces. Stud. Geophys. Geod. **23**, 131–137, 1979

Hubral, P.: Wave front curvatures in 3-D laterally inhomogeneous media with curved interfaces. Geophysics **45**, 905–913, 1980

Hubral, P.: Computing true amplitude reflections in a laterally inhomogeneous Earth. Geophysics **48**, 1051–1062, 1983

Hubral, P., Krey, Th.: Interval velocities from seismic reflection measurements. SEG Monograph Series No. 3. Tulsa: SEG 1980

Jacob, K.H.: Three-dimensional seismic ray tracing in a laterally heterogeneous spherical Earth. J. Geophys. Res. **75**, 6675–6689, 1970

Julian, B.R., Gubbins, D.: Three-dimensional seismic ray tracing. J. Geophys. **43**, 95–113, 1977

Karal, F.C., Keller, J.B.: Elastic wave propagation in homogeneous and inhomogeneous media. J. Acoust. Soc. Am. **31**, 694–705, 1959

Kirpichnikova, N.Y., Popov, M.M.: Reflection of space-time ray amplitudes from a moving boundary. In: Mathematical problems of the theory of propagation of waves (in Russian), Vol. 13, V.M. Babich, ed.: pp. 72–88. Leningrad: Nauka 1983

Klem-Musatov, K.D., Aizenberg, A.M.: The ray method of the theory of edge waves. Geophys. J.R. Astron. Soc. **79**, 35–50, 1984

Klimeš, L.: Computation of seismic wave fields in 3-D media by the Gaussian beam method. Program SW84 (in Czech). Research Report No. 68. Prague: Charles University, Institute of Geophysics 1985

Kline, M., Kay, I.W.: Electromagnetic theory and geometrical optics. New York: Interscience 1965

Kravtsov, Yu.A., Orlov, Yu.I.: Geometrical optics of inhomogeneous media (in Russian). Moscow: Nauka 1980

Krebes, E.S, Hron, F.: Ray synthetic seismograms for *SH* waves in aneslastic media. Bull. Seismol. Soc. Am. **70**, 29–46, 1980

Krebes, E.S., Hron, F.: Comparison of synthetic seismograms for anelastic media by asymptotic ray theory and the Thompson-Haskell method. Bull. Seismol. Soc. Am. **71**, 1463–1468, 1981

Langston, C.A., Lee, J.J.: Effects of structure geometry on strong ground motions: The Duwamish River Valley, Seattle, Washington. Bull. Seismol. Soc. Am. **73**, 1851–1863, 1983

Lee, J.J., Langston, C.A.: Three-dimensional ray tracing and the method of principal curvature for geometrical spreading. Bull. Seismol. Soc. Am. **73**, 765–780, 1983a

Lee, J.J., Langston, C.A.: Wave propagation in a three-dimensional circular basin. Bull. Seismol. Soc. Am. **73**, 1637–1653, 1983b

Lee, W.H.K., Stewart, S.W.: Principles and applications of microearthquake networks. New York: Academic Press 1981

Madariaga, R., Bernard, P.: Ray theoretical strong motion synthesis. J. Geophys. **58**, 73–81, 1985

Marks, L.W., Hron, F.: Calculation of synthetic seismograms in laterally inhomogeneous media. Geophysics **45**, 509–510, 1980

Matveeva, N.N.: Direct and inverse problems for structures with vertically inhomogeneous layered blocks. In: Numerical methods in seismic investigations (in Russian), A.S. Alekseyev, ed.: pp. 14–19. Novosibirsk: Nauka 1983

May, B.T., Hron, F.: Synthetic seismic sections of typical petroleum traps. Geophysics **43**, 1119–1147, 1978

McMechan, G.A., Mooney, W.D.: Asymptotic ray theory and synthetic seismograms for laterally varying structure: Theory and application to the Imperial Valley, California. Bull. Seismol. Soc. Am. **70**, 2021–2035, 1980

Misner, C.W., Thorne, K.S., Wheeler, J.A.: Gravitation. San Francisco: Freeman 1973

Mooney, W.D. (ed): Proceedings of the Workshop on interpretation of seismic wave propagation in laterally heterogeneous structures, Einsiedeln 1983. Menlo Park: U.S. Geological Survey 1985

Müller, G.: Efficient calculation of Gaussian beam seismograms for two-dimensional inhomogeneous media. Geophys. J.R. Astron. Soc. **79**, 153–166, 1984

Pereyra, V., Lee, W.H.K., Keller, H.B.: Solving two-point seismic ray tracing problems in a heterogeneous medium. Part I. A general adaptive finite difference method. Bull. Seismol. Soc. Am. **70**, 79–99, 1980

Petrashen, G.I., Kashtan, B.M.: Theory of body-wave propagation in inhomogeneous anisotropic media. Geophys. J.R. Astron. Soc. **76**, 29–39, 1984

Popov, M.M.: On a method of computation of geometrical spreading in inhomogeneous medium containing interfaces (in Russian). Doklady Akad. Nauk SSSR **237**, 1059–1062, 1977

Popov, M.M., Pšenčík, I.: Ray amplitudes in inhomogeneous media with curved interfaces. In: Geofys. sb., Vol. **24**, A. Zátopek, ed.: pp. 118–129. Praha: Academia 1978a

Popov, M.M., Pšenčík, I.: Computation of ray amplitudes in inhomogeneous media with curved interfaces. Stud. Geophys. Geod. **22**, 248–258, 1978b

Popov, M.M., Tyurikov, L.G.: On two approaches to the evaluation of geometrical spreading in inhomogeneous isotropic media. In: Problems of the dynamic theory of propagation of seismic waves (in Russian), Vol. 20, G.I. Petrashen, ed.: pp. 61–68. Leningrad: Nauka 1981

Pšenčík, I.: Ray amplitudes of compressional shear and converted waves in three-dimensional laterally inhomogeneous media with curved interfaces. J. Geophys. **45**, 381–390, 1979

Pšenčík, I.: Solution of the direct seismic problem for laterally inhomogeneous media by the ray method. In: Numerical methods in seismic investigations (in Russian), A.S. Alekseyev, ed.: pp. 5–13. Novosibirsk: Nauka 1983

Ratnikova, L.I.: Methods of computation of seismic waves in thin-layered media (in Russian). Moscow: Nauka 1973

Shah, P.M.: Ray tracing in three dimensions. Geophysics **38**, 600–604, 1973a

Shah, P.M.: Use of wavefront curvature to relate seismic data with subsurface parameters. Geophysics **38**, 812–825, 1973b

Sharafutdinov, V.A.: On the geometrical spreading. In: Mathematical methods of the interpretation of geophysical observations (in Russian), A.S. Alekseyev, ed.: pp. 161–174. Novosibirsk: Acad. Sci. USSR, Computing Center 1979

Sierra Geophysics Brochure Package. Sierra Geophysics: Redmond, n.d.

Sorrels, G.G., Crowley, J.B., Veith, K.F.: Methods for computing ray paths in complex geological structures. Bull. Seismol. Soc. Am. **61**, 27–53, 1971

Spence, G.D., Whittall, K.P., Clowes, R.M.: Practical synthetic seismograms for laterally varying media calculated by asymptotic ray theory. Bull. Seismol. Soc. Am. **74**, 1209–1223, 1984

Spudich, P., Frazer, L.N.: Use of ray theory to calculate high-frequency radiation from earthquake sources having spatially

variable rupture velocity and stress drop. Bull. Seismol. Soc. Am. **74**, 2061–2082, 1984

Synge, J.L.: Relativity: The general theory. Amsterdam: North Holland Publ. Co. 1960

Synge, J.L., Schild, A.: Tensor calculus. Toronto: Univ. of Toronto Press 1952

Ursin, B.: Quadratic wavefront and travel time approximation in inhomogeneous layered media with curved interfaces. Geophysics **47**, 1012–1021, 1982a

Ursin, B.: A new derivation of the wavefront curvature transformation at an interface between two inhomogeneous media. Geophys. Prospecting **30**, 569–579, 1982b

Vlaar, N.J.: Ray theory for an anisotropic inhomogeneous elastic medium. Bull. Seismol. Soc. Am. **58**, 2053–2072, 1968

Wesson, R.L.: A time integration method for computation of the intensities of seismic rays. Bull. Seismol. Soc. Am. **60**, 307–316, 1970

Wesson, R.L.: Travel-time inversion for laterally inhomogeneous crustal velocity models. Bull. Seismol. Soc. Am. **61**, 729–746, 1971

Whittall, K.P., Clowes, R.M.: A simple, efficient method for the calculation of travel times and ray paths in laterally inhomogeneous media. J. Can. Soc. Exp. Geoophys. **15**, 21–29, 1979

Will, M.: Calculation of travel-times and ray paths for lateral inhomogeneous media. In: Exploration seismology in Central Europe: Data and results, P. Giese, C. Prodehl and A. Stein, eds.: pp. 168–177. Berlin: Springer Verlag 1976

Yacoub, N.K., Scott, J.H., McKeown, F.A.: Computer ray tracing through complex geological models for ground motion studies. Geophysics **35**, 586–602, 1970

Young, R.M.: The interaction of elastic waves with inhomogeneous media. PhD Thesis. Wellington: Victoria Univ., Mathematics Dept. 1985

Young, T.K., Monash, C.B., Turpening, R.M: Computer modeling of vertical seismic profiling. CGG Technical Series No. 532.83.08. Presented at the 53rd SEG Meeting, Las Vegas 1983

Zilkha, S., Sullivan, D.H., Adams, W.D., Coplin, T.L.: Three-dimensional forward and inverse ray tracing modeling. Symposium on Geophysical Modeling. Houston: Geophysical Society of Houston 1983

Received February 20, 1985; revised May 25, 1985
Accepted June 14, 1985